AN ATLAS OF Hα-EMITTING REGIONS IN M 33: A SYSTEMATIC SEARCH FOR SS433 STAR CANDIDATES

Daniela Calzetti, Anne L. Kinney

Space Telescope Science Institute

3700 San Martin Drive

Baltimore, MD 21218

Holland Ford

Johns Hopkins University

Dept. of Physics and Astronomy

Homewood Campus

Baltimore MD 21218

Jesse Doggett, Knox S. Long

Space Telescope Science Institute

To be published in the *A. J.*

Received 18 July 1995 ; Accepted 14 August 1995

ABSTRACT

We report finding charts and accurate positions for 432 compact Hα emitting regions in the Local Group galaxy M 33 (NGC 598), in an effort to isolate candidates for an SS433-like stellar system. The objects were extracted from narrow band images, centered in the rest-frame Hα(λ6563Å) and in the red continuum at 6100 Å. The atlas is complete down to V$\simeq$20 and includes 279 compact HII regions and 153 line emitting point-like sources. The point-like sources undoubtedly include a variety of objects: very small HII regions, early type stars with intense stellar winds, and Wolf-Rayet stars, but should also contain objects with the characteristics of SS433. This extensive survey of compact Hα regions in M 33 is a first step towards the identification of peculiar stellar systems like SS433 in external galaxies.

1. INTRODUCTION

The stellar system SS433 is unique in our Galaxy, and has been the subject of many studies aimed at understanding its nature and the reasons for its peculiarity (see reviews by Margon 1984, Margon & Anderson 1989, and Vermeulen 1993). SS433 is an eclipsing binary system likely to consist of a compact object surrounded by an accretion disk and of an early type star undergoing copious mass loss. Its most remarkable characteristic is the highly collimated anti-parallel relativistic jets ($v = 0.26c$) emerging from the compact object, fueled by the accretion disk, and precessing with a period of about 164 days. At optical wavelengths, the binary system is associated with a 'stationary spectrum' (Margon *et al.* 1979) which shows a red continuum, mostly due to the heavy intervening interstellar absorption ($A_V \sim 8$ mag), and broad and intense Balmer and He I emission lines. These broad lines are the signature of a system dominated by an accretion disk. The equivalent widths of the emission lines are highly variable and the EW of the Hα line can exceed 500 Å. The jets are associated with Doppler red- and blue-shifted Balmer and He I emission lines which move across the spectrum up to $z \sim 0.2$, with a period of 164 days, and are variable in intensity, though fainter than the stationary lines. SS433 is a bright radio source, with a typical quiescent flux density of 0.5 Jy at 5 GHz (Vermeulen 1993), but is only a moderately bright X-ray source, with a luminosity $L_X \sim 10^{35}$ erg s^{-1} in the energy range 0.5–3 keV (Seward *et al.* 1980).

Although SS433 is unmatched by other systems in our Galaxy, a handful of Galactic X-ray sources with jet-like radio lobes may constitute a class of objects similar to SS433 (see Spencer *et al.* 1986, Vermeulen 1993, Tingay *et al.* 1995). However, their behavior is not as extreme or they have only episodic radio and X-ray outbursts. Because of the high extinction affecting the line of sight towards SS433, a detailed study of the environment surrounding the binary system is difficult; little can thus be inferred about the progenitors of the system. SS433 is a Population I object associated with the supernova remnant W50 (Kirshner & Chevalier 1980, Margon 1984, Elston & Baum 1987), which suggests that the SS433 phenomenon is related to the final stages of the stellar evolution.

Finding SS433-like objects in other galaxies would help to unravel the mysteries of the phenomenon. The study of similar objects would clarify the physical mechanisms which lead to the creation of such systems, constrain the type and fraction of binaries which undergo an SS433 phase, and reveal the properties of the environments which harbor SS433-like binaries. The relativistic, collimated jets of SS433 are remarkably similar to the ultrarelativistic jets originating from the nuclei of active galaxies. If SS433-like systems in external galaxies are less obscured than the Galactic prototype, the study of those objects may yield the answer to the mechanism which is at the basis of the jet phenomenon, not only in binary systems, but possibly also in AGNs. And finally, SS433-like systems would provide information on the influence of the jets on the surrounding ISM: given the energetics of the jets in SS433, such stars may induce new star formation in much the way supernovae have been proposed to do. mission cannot be detected.

SS433 is intrisically luminous ($M_V = -7$ or brighter, see Margon 1984), making searches for analogous objects in nearby galaxies feasible.

Given the rarity of the phenomenon, large galaxies offer a better chance to find binary systems with similar characteristics; the two nearby spirals in the Local Group, M 31 and M 33, are therefore suitable for this study. SS433 has a high mass progenitor, which suggests that M 33 (dist=795 kpc, van der Bergh 1991), and v=$-$179 km s^{-1}) is the first place to look, since it has a higher star formation rate than M 31. M 33 is also more face-on than M 31, implying a smaller dust extinction towards the central regions of the galaxy.

The first step towards the identification of SS433-like objects in an external galaxy is the compilation of a suitable list of candidates from a survey. Among the marking features of SS433 are the intense and broad emission lines of the stationary spectrum, such as the Hα line, which has a typical equivalent width ranging from 400 to 500 Å, and a FWHM$\sim$50 Å (cf. Margon *et al.* 1984, Murdin, Clark & Martin 1980). By comparing images of M 33 taken in the rest frame Hα band with images taken in the adjacent continuum, we are able to flag all the stellar sources showing excess emission in the Hα line. This is an efficient method for collecting candidates, because images cover extended regions of a galaxy and increase the chance of including rare objects like SS433 in the sample. However, the technique does not discriminate SS433 systems from other point-like Hα emitting objects, such as early type stars with intense winds, W-R stars, and compact HII regions, although stars do tend to have small Hα EWs (*e.g.* Conti 1974, Conti, Leep & Perry 1983).

For completeness, we have also compiled a list of stellar sources surrounded by extended Hα emission. Although SS433 is not known to be in a OB association or in an HII complex, it has high mass progenitors and lives in a Population I environment. Random motions carry some massive stars out of OB associations before they become supernovae; Huang (1987) found that 25 out of 29 Type II supernovae are associated with, but not embedded in, HII regions and OB associations. If an SS433-like system is present in M 33, it may be found in an environment with ongoing star formation. Small HII regions may in principle conceal line emitting stars, though most of the objects in our list are likely to be simply hot stars embedded in compact HII regions.

The final result is a comprehensive survey of compact Hα emitting objects in M 33, which includes both small HII regions and point-like sources, complete down to V$\sim$20. For all the objects we provide accurate positions and finding charts (see section 2). Radio jets in SS433-like stars are produced in the presence of mass transfer in a binary system; such systems will tend to be detected as X-ray sources (cf. Vermeulen 1993). In addition, SS433 is bright in the radio and is associated with a supernova remnant. We analyze in section 3 possible coincidences of our candidates' positions with known SNRs, X-ray and radio sources in M 33. The summary is given in section 4.

2. DATA AND SELECTION CRITERIA

2.1. The Data

For this project, images of M 33 in Hα and in a narrow band continuum region around 6100 Å were employed. The images were obtained by Long *et al.* (1990) as part of a project for the search of supernova remnants in M 33. They cover about 70% of the most active region in M 33, excluding only the outer arms. Here we give a brief summary of the observational material. A more detailed description can be found in the paper by Long *et al.* (1990).

All the images were obtained at the prime focus of the Kitt Peak 4 meter telescope, during two observing runs, in 1986 and 1987. The 800×800 TI-2 CCD employed covered a field of view of 3.86 arcmin^2 with a scale of 0.30 arcsec pix^{-1}. A mosaic of 19 images in each filter of the central region of M 33 was built (see Fig. 1). The 19 images are spaced by 3.5′, ensuring an overlap by at least 30″ on each side. As shown in Fig. 1, the fields are labelled alphabetically, from 'a' to 's', to help identify the candidates on the finding charts.

The interference filters used for the narrow band images were slightly different during the 1986 and 1987 runs. In 1986, the Hα filter (on-band) was centered at 6575 Å, with FWHM=52 Å, and the continuum filter (off-band) was centered at 6100 Å, with FWHM=150 Å. In 1987, the on-band filter was centered at 6563 Å, with FWHM=32 Å, and the off-band filter was centered at 6097 Å, with FWHM=130 Å. Exposure times were 1200 s for the on-band filter and ranged from 200 s to 1000 s for the off-band filter. The seeing varied in the range 0″.8–2″.1, which, at the distance of M 33, corresponds to a spatial scale 3.1–8.1 pc. As a result, we are unable to distinguish small size HII regions from isolated stars.

2.2. The Selection of the Candidates

In each of the 19 fields, the Hα emission line stars were identified by comparing the on-band and off-band images, and by marking the objects for which the emission in the Hα filter appeared brighter than the emission in the continuum filter.

The first step in the procedure was to scale the two sets of images to a common value and set the same zero-point. An excellent match between the sequential pairs of images was achieved by measuring and rescaling the counts of 5 to 15 bright foreground Galactic stars in each field, which are unlikely to have intrinsic Hα emission. The small change in the color of the stars from 6100 Å to $\sim$6570 Å was neglected. The on-band and off-band images for each field were then electronically blinked and

point-like sources were flagged as Hα emitters if they appeared to be brighter in the on-band image than in the off-band image. A total of 153 'emission-line candidates' were identified. Sources which appeared as point-like objects in the off-band images, and were projected onto extended nebulosity in the on-band images were also flagged. These objects are likely to be physically associated with the extended Hα emission, and we will refer to them as 'embedded candidates'. A total of 279 such objects was found in the 19 fields. On-band and off-band fluxes of the 432 candidates were measured by fitting a gaussian to each source and summing the counts under the curve.

The conversion from counts to flux was obtained by rescaling for the counts of calibration standards, after correction for the atmospheric extinction. Uncertainties on the flux measurements are of the order of 10% at the bright end, and become increasingly larger for dimmer sources. The flux in the Hα line was calculated for each object by subtracting the contribution of the off-band continuum from the on-band fluxes. Color corrections between 6100 Å and ~6570 Å were assumed to be negligible. This assumption is reasonable for stars with spectral types A or earlier.

The basic results of the survey are presented in Table 1 and Table 2, for the emission-line and the embedded sources, respectively. The emission-line stars are rank ordered according to the equivalent width of the Hα emission (EW(Hα)), obtained as the ratio between the flux in the Hα line and the continuum at 6100 Å. The embedded stars are rank ordered according to the V magnitude. The V magnitude is derived from the continuum at 6100 Å, assuming a V zero-point $f_{V(0)}=3.64\times10^{-9}$ erg s^{-1} cm^{-2} Å^{-1} and negligible color correction between 6100Å and 5500Å. Fluxes below 4×10^{-19} erg s^{-1} cm^{-2} Å^{-1} in the 6100 Å filter (V>25) are too faint to be reliably measured with our method; in these cases the value of the V magnitude has been omitted. Other information contained in the Tables are: the identification of the field the source belongs to, the identification of the source within the field, and the 1950 equatorial coordinates. The sources are labelled with a number followed by a 'e' in the case of the emission-line candidates or by a 'b' in the case of the embedded candidates.

Accurate positions for the candidates were measured by determining plate solutions for the 19 fields using the HST Guide Star Selection System (GSSS) and the GSSS Astrometric Support Program (GASP). An iterative two-dimensional gaussian fit was usually employed to determine x-y pixel positions for the objects in each field. Some regions of M 33 have highly variable background, which made the two-dimensional fit diverge; in those cases a one-dimensional fit along the x and the y coordinates was employed. For each of our fields, 20 to 30 bright isolated stars in common with the GSSS plates were used to convert the x-y positions into equatorial coordinates.

A linear least square fit was applied to both the coordinates and the x-y positions of the candidates to derive plate solutions for our images. Only linear terms in the model were needed and there were no systematic changes of residuals across the images. The residuals to the plate solutions indicate that our relative coordinates are accurate to ~0.″4. The 1950 equatorial coordinates listed in Tables 1 and 2 are derived from the plate solutions. The positions of the 432 candidates in the 19 fields are shown in Figs. 2a to 2s.

For an easy access to the data, the postscript files of Tables 1 and 2 will be made available via anonymous ftp at the node ftp.stsci.edu, under the directory outside-access/out.going.

3. DISCUSSION

The peak of the flux distribution at 6100 Å is approximately the same for all the plates independently of the exposure time (ranging from 200 s to 1000 s).

We adopt the peak as our completeness limit in the continuum, namely $\sim 3\times10^{-17}$ erg s^{-1} cm^{-2} Å^{-1}. Assessing a more rigorous limit for the survey is difficult, since the "human factor" is important here for recognizing objects with the required characteristics, expecially at the faint end of the flux distribution. This flux limit is equivalent to a magnitude $V \sim 20$, which translates into an absolute magnitude $M_V \simeq -4.5$ at the distance of M 33. If a system like SS433 is present in M 33, it is likely to be among our candidates even if it is affected by moderate reddening or if it is a couple of magnitudes fainter than the Galactic SS433. The uncertainties in the flux measurements, of the order of 10–15%, translate into a minimum detectable EW(Hα)≃20-25 Å for the emission-line candidates. Therefore, an SS433-like system can be present in this survey even if its stationary Hα line emission is a factor 20 weaker than its Galactic counterpart. Of the 153 objects listed in Table 1, the top 86 have EW(Hα)≥20 Å. The remaining 67, although they still show excess emission in the on-band filter relative to the off-band filter, can be considered marginal candidates. Indeed, we cannot discriminate between blue stars with a weak Hα

emission and red stars (*e.g.* M supergiants) with the 6100 Å continuum fainter than the 6570 Å continuum.

The first two objects in Table 1 have EW(Hα)> 1000 Å, much larger than the Galactic SS433. Such values for the EW are compatible with nebular emission from HII regions. Indeed, the fields b and e, where the two candidates are located, were observed with a seeing of 1".7 (see Long *et al.* 1990), which corresponds to a linear scale of 6.6 pc; this is larger than the tipical size of nebulae ionized by single O stars (cf. Osterbrock 1989).

The positions of our candidates have been cross-correlated with known Wolf-Rayet stars (Massey & Conti 1983, Massey *et al.* 1987) to check for common objects between the two samples. Given the uncertainties in our candidates' positions, $\sim 0''.4$, and in the W-R coordinates, 2" from Massey & Conti (1983) and $\approx$1" from Massey *et al.* (1987), we have chosen to consider potential coincidences for all sources located within 3" of a W-R star. This provides a list of 2 emission-line objects and 6 embedded objects (see Table 3). Among these, our source 96b and the W-R star MCMS04 are certainly the same object. The other 7 "coincidences" cannot be assessed by simple visual inspection of the Massey *et al.* (1987) finding charts, due to the crowding of the fields. It is plausible that the candidates lying at the border of our correlation radius, namely 25e, 276b, and 277b, are not actual coincidences, but this remains to be confirmed.

The association of SS433 with the SNR W50 may have a physical origin (Elston & Baum 1987): the supernova explosion which created W50 could have also created SS433. In this light, we have searched for positional coincidences between our candidates and known SNRs in M 33 (Long *et al.* 1990, Gordon *et al.* 1994, Gordon *et al.* 1995). Using the sizes of the SNRs reported by Long *et al.* 1990 and Gordon *et al.* 1994, we have listed in Table 4 all the candidates which are located within or close to the region of the sky occupied by a SNR. The coincidences listed in the Table are purely geometrical, and the existence of physical associations between the candidates and the SNRs cannot be assessed at this stage.

Although SS433 is an X-ray source of moderate intensity, SS433-like binary systems have a high probability to be bright X-ray sources (Vermeulen 1993). We have cross-correlated our candidates positions with the point sources detected by the ROSAT Position Sensitive Proportional Counter (PSPC, Long *et al.* 1995) and by the ROSAT High-Resolution Imager (HRI, Schulman & Bregman 1995), searching for coincidences between the Hα emitting objects and the X-ray sources in M 33. The deepest X-ray image of M 33, obtained with the ROSAT PSPC, has a detection limit of $\sim 7\times10^{35}$ erg s^{-1} for the energy band 0.1-2.4 keV, which is about one order of magnitude larger than the SS433 luminosity (Long *et al.* 1995). However, the range of X-ray luminosities one should expect for SS433-like systems is unknown, and correlations between optical and X-ray sources may still reveal the presence of interesting objects. The angular resolution is $\sim$20" for the PSPC (Long *et al.* 1995) and $\sim$4" for the HRI. To allow for uncertainties in the two ROSAT surveys, we investigate all the X-ray sources located within 20" of our candidates (see Table 4). It can be readily seen from Table 4 that most of the "coincidences" have already a plausible identification, other than the Hα sources (Long *et al.* 1995, Schulman & Bregman 1995): the X-ray emission of RP05, RP22, RP35, and RP36 can be attributed to SNRs; the X-ray source RP28=RH16 is associated with the nucleus of M 33; and RP24=RH14 is presumably too far from the emission-line star 86e. However, there are three interesting cases. RP21=RH12 is an eclipsing X-ray binary (Schulman *et al.* 1993) and is located at a distance of only 6".4 from our candidate 99b. RP14 and RP30 are probably also X-ray binaries, given their hard X-ray spectrum (Long *et al.* 1995), and may be associated with some of the candidates in our list, but a chance coincidence cannot be excluded.

If SS433 were at the distance of M 33, its radio flux density would be about 2.5 mJy at 5 GHz. The deepest radio surveys currently available are from VLA observations and have detection limits between 0.1 and 0.5 mJy both at 1.5 GHz and 5 GHz (Gordon *et al.* 1995), implying that a source with the SS433 radio luminosity would be easily detected. Table 5 lists all the radio sources located within 3" from our candidates. Gordon *et al.* (1995) provide optical identification for most of the radio sources in Table 5; they are SNRs or HII regions from the catalog of Boulesteix *et al.* (1974). Only two candidates, 33b and 184b, do not have an obvious optical counterpart. For these sources, the radio fluxes at 5 GHz are 0.1 and 0.4 mJy, respectively.

4. SUMMARY

Using images obtained with interference filters centered on the Hα line and the continuum at 6100 Å, we have compiled a list of Hα emitting compact regions and isolated stellar sources, which may be candidates for an SS433-like system in M 33. To be included in our sample, an object had to satisfy one of two selection criteria: 1) show a point-like Hα emission in excess of the continuum

emission (emission-line candidates); 2) be a point-like continuum source projected onto extended Hα emission (embedded candidates). Most of the sources will turn out to be compact HII regions, although massive peculiar stars and, possibly, an SS433-like system may be in the list. The emission-line stellar sources are the best candidates for an SS433 system, but we cannot exclude the possibility that there may be line emitting stars concealed in compact HII regions. For all the objects in our atlas, we provide coordinates precise to 0".4 and finding charts. Given that SS433 is a radio and X-ray source and is associated with a SNR, our candidates have been searched for positional coincidence with SNRs, and radio and X-ray point sources in M 33. Some of our candidates are indeed located very close to a few of these objects, but no secure association could be recognized. Follow-up spectroscopy is clearly required to identify the nature of the candidates in our atlas.

Acknowledgements

The authors thank Shawn Gordon for providing his list of radio sources in M 33 prior to publication, and William Blair for useful comments and a critical reading of the manuscript. D. C. acknowledges support from the NASA Grant NAGW-1485 during this research. K. S. L.'s work on M 33 has been supported by the NASA Grant NAG5-1539.

REFERENCES

Boulesteix, J., Courtèx, G., Laval, A., Monnet, G., & Petit, H. 1974, *A&A*, **37**, 33

Conti, P. S. 1974, *Ap. J.*, **187**, 539

Conti, P. S., Leep, E. M., & Perry, D. N. 1983, *Ap. J.*, **268**, 228

Elston, R., & Baum, S. 1987, *A. J.*, **94**, 1633

Long, K. S., Blair, W. P., Kirshner, R. P., & Winkler, P. F. 1990, *ApJS*, **72**, 61

Long, K. S., Blair, W. P., Charles, P. A., & Gordon, S. M. 1995, in prep.

Gordon, S. M., Kirshner, R. P., Duric, N., & Long, K. S. 1994, *Ap. J.*, **418**, 743

Gordon, S. M., Kirshner, R. P., Duric, N., & Long, K. S. 1995, in prep. Huang, Y.-L. 1987, PASP, **99**, 461

Kirshner, R. P., & Chevalier, R. A. 1980, *Ap. J.*, **242**, L77

Margon, B. 1984, *ARA&A*,**22**, 507

Margon, B., Anderson, S. F., Aller, L. H., Downes, R. A., & Keyes, C. D. 1984, *Ap. J.*, **281**, 313

Margon, B., & Anderson, S. F. 1989, *Ap. J.*, **347**, 448

Margon, B., Ford, H. C., Grandi, S. A., & Stone, R. P. S. 1979, *Ap. J.*, **233**, L63

Massey, P., & Conti, P. S. 1983, *Ap. J.*, **273**, 576

Massey, P., Conti, P. S., Moffat, A. F. J., & Shara, M. 1987, PASP, **99**, 816

Murdin, P., Clark, D. H., & Martin, P. G. 1980, *M.N.R.A.S.*, **193**, 135

Osterbrock, D. E. 1989, Astrophysics of Gaseous Nebulae and Active Galactic Nuclei, University Science Books (Mint Valley, CA)

Seward, F., Grindlay, J., Seaquist, E., & Gilmore, W. 1980, *Nature*, **287**, 806

Schulman, E., & Bregman, J. N. 1995, *Ap. J.*, **441**, 568

Schulman, E., Bregman, J. N., Collura, A., Reale, F., & Peres, G. 1993, *Ap. J.*, **418**, L67

Spencer, R. E., Swinney, R. W., Johnston, K. J., & Hjeliming, R. M. 1986, *Ap. J.*, **309**, 694

Tingay, S. J., *et al.* 1995, *Nature*, **374**, 141

van der Bergh, S. 1991, PASP, **103**, 609

Vermeulen, R., 1993, in *Astrophysical Jets*, eds. D. Burgarella, M. Livio, & C. O'Dea, Camdridge University Press, 241

TABLE 1. EMISSION-LINE CANDIDATES

#	Field	ID	r.a. (1950)	dec. (1950)	EW(Hα)[a]	V[b]
1	b	95e	1:30:59.190	30:24:13.84	1763.5	19.18
2	e	73e	1:30:48.720	30:24:12.64	1312.5	20.13
3	h	59e	1:30:45.290	30:16:02.69	663.9	20.66
4	n	68e	1:30:47.580	30:27:39.42	603.2	21.21
5	o	152e	1:31:33.060	30:17:16.21	396.1	21.16
6	r	20e	1:30:23.410	30:20:33.62	377.6	22.03
7	b	100e	1:31:00.870	30:26:04.72	375.2	17.23
8	m	101e	1:31:00.880	30:26:04.72	285.0	17.22
9	h	90e	1:30:55.440	30:16:39.14	250.9	18.87
10	g	71e	1:30:48.240	30:21:19.76	245.0	19.35
11	c	89e	1:30:55.430	30:16:39.26	226.4	18.59
12	o	151e	1:31:33.020	30:17:21.02	203.9	21.84
13	o	149e	1:31:31.980	30:17:23.18	183.1	21.73
14	s	19e	1:30:22.720	30:29:40.34	159.8	20.43
15	c	96e	1:30:59.460	30:17:26.05	147.9	20.25
16	m	120e	1:31:11.410	30:29:15.58	145.4	19.12
17	o	153e	1:31:36.860	30:19:03.92	144.7	19.54
18	m	110e	1:31:08.070	30:28:04.14	142.7	20.34
19	f	26e	1:30:26.790	30:24:29.18	130.1	20.69
20	k	117e	1:31:09.980	30:26:04.44	128.2	20.24
21	n	81e	1:30:52.600	30:28:44.97	114.6	20.53
22	k	123e	1:31:12.090	30:23:54.01	112.8	20.20
23	g	45e	1:30:37.490	30:20:27.88	109.8	20.52
24	l	130e	1:31:17.370	30:26:26.26	109.1	16.76
25	i	41e	1:30:34.840	30:13:41.26	104.3	20.38
26	c	85e	1:30:53.670	30:17:33.93	99.0	18.76
27	k	118e	1:31:11.180	30:22:43.09	97.5	20.73
28	p	113e	1:31:09.510	30:17:20.09	96.6	20.75
29	h	84e	1:30:53.660	30:17:34.18	91.6	18.56
30	q	4e	1:30:18.580	30:15:53.63	85.7	19.50
31	a	3e	1:30:05.290	30:22:42.02	85.2	20.27
32	s	25e	1:30:26.140	30:29:40.93	84.9	20.30
33	k	126e	1:31:14.790	30:25:15.63	83.3	19.17
34	k	134e	1:31:19.920	30:23:25.55	82.4	20.74
35	n	75e	1:30:50.300	30:28:49.78	80.3	20.36
36	i	22e	1:30:25.280	30:14:30.09	78.0	20.28
37	f	27e	1:30:26.900	30:24:18.68	71.5	20.88
38	e	63e	1:30:45.860	30:22:25.78	66.2	20.68
39	a	12e	1:30:21.260	30:23:13.77	64.1	19.91
40	i	48e	1:30:38.320	30:15:06.90	63.2	18.45
41	m	107e	1:31:03.190	30:28:30.10	62.4	19.65
42	o	144e	1:31:26.520	30:18:39.51	61.3	19.60
43	i	16e	1:30:21.720	30:11:51.96	61.0	19.95
44	p	138e	1:31:24.810	30:15:28.50	57.0	20.96
45	h	70e	1:30:48.240	30:18:06.75	56.9	19.30
46	c	109e	1:31:05.680	30:17:27.28	56.8	19.18
47	g	62e	1:30:45.850	30:22:25.79	51.0	20.65
48	o	143e	1:31:26.490	30:15:26.68	49.1	20.06
49	l	121e	1:31:11.750	30:26:03.91	47.1	20.67

TABLE 1—*Continued*

#	Field	ID	r.a. (1950)	dec. (1950)	EW(Hα)[a]	V[b]
50	h	57e	1:30:44.400	30:16:27.28	45.9	19.77
51	l	136e	1:31:22.630	30:26:58.35	45.7	20.90
52	l	119e	1:31:11.380	30:29:15.69	45.4	19.76
53	i	31e	1:30:29.070	30:14:24.01	43.0	20.01
54	g	78e	1:30:51.100	30:18:55.70	41.5	19.23
55	s	49e	1:30:38.240	30:26:03.95	37.2	20.87
56	s	37e	1:30:30.520	30:28:54.26	36.7	21.05
57	s	38e	1:30:31.030	30:27:40.27	36.0	19.82
58	s	14e	1:30:21.390	30:28:11.38	33.9	20.36
59	g	54e	1:30:41.950	30:19:40.74	33.8	19.42
60	g	53e	1:30:41.160	30:19:48.20	32.6	19.60
61	j	146e	1:31:26.830	30:21:21.07	32.4	18.10
62	n	69e	1:30:48.120	30:28:51.40	31.7	20.88
63	b	99e	1:31:00.050	30:22:47.43	31.3	16.76
64	e	77e	1:30:50.640	30:25:10.11	31.1	19.47
65	i	18e	1:30:22.470	30:11:50.89	30.3	20.47
66	m	98e	1:30:59.500	30:26:49.59	30.2	20.06
67	o	139e	1:31:25.010	30:18:22.14	29.7	19.35
68	h	51e	1:30:39.810	30:15:35.49	29.2	19.70
69	b	106e	1:31:03.210	30:23:47.92	28.3	16.33
70	g	50e	1:30:39.040	30:19:24.54	27.6	20.37
71	n	60e	1:30:45.400	30:29:23.24	26.9	19.76
72	e	66e	1:30:46.460	30:23:14.47	25.1	18.87
73	g	74e	1:30:49.830	30:19:44.08	24.6	19.89
74	m	97e	1:30:59.440	30:29:04.19	24.5	19.70
75	a	2e	1:30:04.170	30:23:32.75	22.5	19.82
76	s	47e	1:30:38.080	30:26:16.81	22.3	21.18
77	g	88e	1:30:54.210	30:19:16.10	22.1	19.32
78	h	65e	1:30:46.450	30:15:29.52	21.3	19.80
79	g	44e	1:30:37.420	30:19:17.48	21.1	20.18
80	g	83e	1:30:53.230	30:18:53.41	21.0	19.94
81	s	32e	1:30:29.150	30:26:53.91	20.9	21.04
82	g	46e	1:30:37.500	30:21:07.17	20.5	20.11
83	g	58e	1:30:44.430	30:19:57.72	20.5	20.18
84	c	102e	1:31:01.470	30:17:08.54	20.4	18.20
85	a	5e	1:30:18.490	30:26:20.59	20.2	19.11
86	f	39e	1:30:32.300	30:25:22.80	20.1	19.57
87	f	40e	1:30:32.800	30:25:49.37	<20	19.26
88	g	82e	1:30:52.920	30:21:13.21	<20	19.91
89	g	76e	1:30:50.630	30:19:30.20	<20	19.07
90	g	43e	1:30:37.180	30:21:21.59	<20	20.11
91	f	30e	1:30:28.590	30:26:06.42	<20	19.99
92	g	87e	1:30:54.170	30:19:29.07	<20	20.02
93	l	145e	1:31:26.670	30:25:53.49	<20	19.48
94	f	29e	1:30:27.290	30:26:08.43	<20	19.02
95	j	127e	1:31:15.650	30:20:12.47	<20	19.63
96	r	42e	1:30:35.990	30:21:38.11	<20	18.13
97	h	64e	1:30:46.140	30:15:18.64	<20	19.48
98	e	67e	1:30:47.210	30:23:41.04	<20	20.09

TABLE 1—*Continued*

#	Field	ID	r.a. (1950)	dec. (1950)	EW(Hα)[a]	V[b]
99	h	79e	1:30:51.100	30:18:55.61	<20	18.90
100	h	80e	1:30:51.300	30:16:09.22	<20	20.23
101	m	116e	1:31:09.960	30:26:04.15	<20	19.27
102	r	21e	1:30:24.750	30:20:35.73	<20	17.58
103	m	93e	1:30:59.070	30:28:04.42	<20	20.19
104	d	111e	1:31:08.640	30:21:56.18	<20	19.09
105	d	104e	1:31:02.280	30:21:18.35	<20	19.22
106	g	72e	1:30:48.520	30:19:06.24	<20	20.27
107	l	115e	1:31:09.800	30:28:33.31	<20	20.11
108	m	92e	1:30:58.270	30:26:33.07	<20	19.63
109	l	140e	1:31:24.990	30:27:32.95	<20	19.73
110	f	23e	1:30:25.470	30:23:10.17	<20	20.05
111	p	137e	1:31:22.790	30:18:47.92	<20	20.00
112	m	91e	1:30:57.370	30:26:03.46	<20	18.81
113	r	33e	1:30:30.030	30:21:19.87	<20	18.76
114	q	34e	1:30:30.120	30:17:34.34	<20	18.10
115	c	108e	1:31:05.680	30:17:01.40	<20	18.12
116	l	141e	1:31:25.250	30:28:47.75	<20	20.39
117	q	8e	1:30:20.660	30:18:08.67	<20	17.99
118	m	94e	1:30:59.110	30:26:42.12	<20	19.91
119	p	124e	1:31:13.260	30:15:41.86	<20	18.90
120	m	103e	1:31:01.590	30:28:41.47	<20	18.70
121	e	61e	1:30:45.460	30:25:33.75	<20	18.28
122	e	55e	1:30:43.430	30:23:05.52	<20	19.30
123	d	105e	1:31:03.000	30:21:14.72	<20	18.31
124	q	6e	1:30:19.650	30:18:46.26	<20	19.44
125	q	35e	1:30:30.210	30:18:25.57	<20	15.29
126	q	28e	1:30:27.240	30:16:44.66	<20	18.38
127	p	135e	1:31:20.120	30:18:53.01	<20	19.10
128	q	7e	1:30:20.450	30:19:28.62	<20	18.63
129	q	24e	1:30:25.920	30:16:38.79	<20	18.61
130	q	17e	1:30:22.100	30:18:58.93	<20	17.21
131	q	13e	1:30:21.460	30:16:38.01	<20	18.43
132	q	10e	1:30:21.040	30:16:05.45	<20	19.03
133	e	86e	1:30:53.770	30:23:25.50	<20	18.92
134	o	150e	1:31:32.970	30:17:18.64	<20	···
135	p	112e	1:31:09.100	30:19:09.73	<20	···
136	r	15e	1:30:21.600	30:20:27.72	<20	···
137	p	133e	1:31:19.400	30:17:23.21	<20	···
138	o	147e	1:31:26.900	30:18:23.69	<20	···
139	l	128e	1:31:15.570	30:29:41.85	<20	···
140	l	125e	1:31:13.520	30:27:07.19	<20	···
141	j	114e	1:31:09.520	30:20:04.64	<20	···
142	o	148e	1:31:29.520	30:18:50.72	<20	···
143	r	36e	1:30:30.480	30:20:07.32	<20	···
144	p	129e	1:31:16.350	30:18:57.46	<20	···
145	p	132e	1:31:19.010	30:18:43.70	<20	···
146	j	122e	1:31:11.970	30:20:56.78	<20	···
147	p	131e	1:31:18.690	30:17:27.24	<20	···

TABLE 1—*Continued*

#	Field	ID	r.a. (1950)	dec. (1950)	EW(Hα)[a]	V[b]
148	k	142e	1:31:25.770	30:25:14.98	<20	···
149	g	52e	1:30:39.790	30:21:11.96	<20	20.38
150	a	9e	1:30:20.960	30:23:17.11	<20	20.84
151	a	11e	1:30:21.130	30:23:22.11	<20	···
152	h	56e	1:30:44.220	30:16:24.79	<20	···
153	a	1e	1:30:03.580	30:22:57.06	<20	19.98

[a]Equivalent width of the Hα line emission, in Å.
[b]V magnitude, calculated from the continuum at 6100 Å.

TABLE 2. Hα-EMBEDDED CANDIDATES

#	Field	ID	r.a. (1950)	dec. (1950)	V[a]
1	d	162b	1:30:55.750	30:21:06.43	14.36
2	d	177b	1:30:56.950	30:21:31.73	16.28
3	f	28b	1:30:22.980	30:23:29.36	16.55
4	b	137b	1:30:53.980	30:23:44.56	16.87
5	d	221b	1:31:09.510	30:20:04.57	16.87
6	d	165b	1:30:55.980	30:20:58.04	16.93
7	g	113b	1:30:47.890	30:21:15.42	17.13
8	d	207b	1:31:06.030	30:19:08.02	17.22
9	f	16b	1:30:21.150	30:23:21.90	17.28
10	d	150b	1:30:55.470	30:20:37.09	17.39
11	d	153b	1:30:55.510	30:20:49.32	17.40
12	c	182b	1:30:58.850	30:17:42.75	17.43
13	n	92b	1:30:44.590	30:26:10.05	17.45
14	f	25b	1:30:22.770	30:23:30.78	17.50
15	m	157b	1:30:55.550	30:29:23.14	17.51
16	b	196b	1:31:03.180	30:23:59.21	17.57
17	e	65b	1:30:39.920	30:25:01.85	17.68
18	b	199b	1:31:04.010	30:23:32.08	17.76
19	c	206b	1:31:04.950	30:17:48.19	17.81
20	b	197b	1:31:03.450	30:23:52.06	17.82
21	b	139b	1:30:54.500	30:23:43.39	17.87
22	h	132b	1:30:53.400	30:17:36.40	17.93
23	n	84b	1:30:44.300	30:26:10.85	18.02
24	d	209b	1:31:06.680	30:18:45.91	18.17
25	n	83b	1:30:44.290	30:26:09.64	18.23
26	d	203b	1:31:04.610	30:20:06.08	18.23
27	f	17b	1:30:21.320	30:23:26.52	18.31
28	d	218b	1:31:08.640	30:20:10.19	18.43
29	d	175b	1:30:56.540	30:20:47.72	18.47
30	b	180b	1:30:58.330	30:23:18.00	18.51

TABLE 2—*Continued*

#	Field	ID	r.a. (1950)	dec. (1950)	V[a]
31	b	141b	1:30:54.510	30:25:34.72	18.59
32	b	202b	1:31:04.390	30:23:29.94	18.65
33	e	66b	1:30:40.600	30:25:01.14	18.65
34	n	149b	1:30:55.300	30:29:10.70	18.76
35	d	213b	1:31:07.240	30:18:59.10	18.84
36	n	160b	1:30:55.570	30:29:10.74	18.84
37	d	185b	1:31:00.520	30:22:08.62	18.93
38	b	184b	1:30:59.590	30:24:25.31	18.94
39	m	169b	1:30:55.920	30:29:27.28	18.97
40	d	142b	1:30:54.610	30:21:22.85	18.97
41	f	60b	1:30:38.120	30:23:47.15	18.98
42	d	226b	1:31:10.030	30:20:23.48	19.01
43	n	159b	1:30:55.570	30:29:23.19	19.11
44	b	126b	1:30:52.590	30:26:27.56	19.17
45	n	74b	1:30:43.770	30:26:13.65	19.17
46	l	251b	1:31:17.450	30:26:32.95	19.18
47	h	68b	1:30:40.960	30:16:23.05	19.23
48	d	208b	1:31:06.410	30:22:19.55	19.29
49	b	190b	1:31:01.640	30:24:24.15	19.30
50	b	200b	1:31:04.050	30:23:57.04	19.36
51	d	201b	1:31:04.390	30:19:58.09	19.36
52	p	265b	1:31:24.990	30:18:22.12	19.36
53	k	240b	1:31:13.230	30:23:20.18	19.38
54	b	187b	1:31:01.440	30:25:58.89	19.38
55	h	133b	1:30:53.420	30:17:52.55	19.39
56	n	155b	1:30:55.460	30:29:15.12	19.41
57	q	36b	1:30:25.580	30:17:12.68	19.45
58	b	195b	1:31:03.030	30:24:04.52	19.46
59	i	18b	1:30:21.970	30:12:10.69	19.48
60	d	227b	1:31:10.110	30:20:30.50	19.48
61	k	238b	1:31:13.000	30:23:28.66	19.49
62	i	19b	1:30:21.950	30:14:34.06	19.50
63	h	99b	1:30:45.290	30:16:46.05	19.51
64	g	104b	1:30:45.740	30:21:08.17	19.51
65	b	198b	1:31:04.000	30:23:41.19	19.52
66	h	62b	1:30:38.420	30:16:31.24	19.54
67	b	191b	1:31:01.880	30:24:43.28	19.54
68	h	117b	1:30:49.880	30:17:14.06	19.54
69	h	89b	1:30:44.630	30:16:38.95	19.55
70	h	130b	1:30:53.140	30:17:39.46	19.55
71	f	59b	1:30:37.880	30:23:19.82	19.56
72	d	172b	1:30:56.210	30:21:21.07	19.58
73	c	179b	1:30:57.710	30:18:10.76	19.58
74	l	236b	1:31:12.460	30:29:35.92	19.64
75	s	38b	1:30:25.740	30:29:37.65	19.65
76	n	98b	1:30:45.180	30:26:39.04	19.66
77	d	210b	1:31:06.870	30:19:00.29	19.66
78	p	264b	1:31:24.810	30:18:23.12	19.68
79	p	267b	1:31:25.160	30:19:13.28	19.69

TABLE 2—*Continued*

#	Field	ID	r.a. (1950)	dec. (1950)	V[a]
80	c	131b	1:30:53.150	30:17:39.21	19.69
81	h	119b	1:30:50.120	30:17:17.43	19.72
82	d	189b	1:31:01.560	30:21:44.57	19.74
83	b	138b	1:30:54.300	30:23:49.82	19.75
84	b	222b	1:31:09.570	30:25:52.02	19.79
85	c	205b	1:31:04.940	30:17:38.43	19.79
86	c	186b	1:31:01.090	30:18:25.46	19.79
87	h	116b	1:30:49.870	30:16:44.40	19.81
88	p	263b	1:31:24.740	30:18:18.43	19.82
89	l	245b	1:31:17.080	30:26:22.57	19.85
90	h	72b	1:30:41.340	30:16:36.12	19.87
91	a	14b	1:30:20.810	30:23:32.68	19.89
92	j	254b	1:31:21.960	30:20:49.56	19.96
93	g	105b	1:30:45.750	30:21:43.33	19.97
94	a	13b	1:30:20.760	30:23:23.58	19.97
95	n	135b	1:30:53.820	30:29:19.00	20.02
96	b	212b	1:31:06.870	30:25:54.23	20.03
97	g	73b	1:30:43.570	30:21:32.90	20.04
98	i	15b	1:30:20.970	30:12:04.63	20.05
99	q	51b	1:30:31.680	30:16:42.20	20.06
100	f	61b	1:30:38.180	30:23:19.84	20.07
101	f	54b	1:30:37.090	30:23:40.42	20.07
102	b	192b	1:31:02.550	30:25:32.73	20.08
103	k	231b	1:31:11.010	30:25:26.18	20.09
104	a	9b	1:30:13.840	30:25:44.26	20.11
105	g	120b	1:30:51.040	30:22:00.30	20.12
106	h	129b	1:30:53.120	30:17:35.97	20.13
107	a	2b	1:30:06.670	30:24:07.61	20.14
108	f	47b	1:30:29.920	30:24:09.67	20.15
109	h	63b	1:30:38.680	30:16:28.40	20.17
110	n	97b	1:30:45.100	30:26:07.96	20.19
111	l	235b	1:31:12.350	30:29:36.74	20.19
112	f	23b	1:30:22.150	30:23:51.73	20.20
113	n	127b	1:30:52.620	30:26:27.37	20.22
114	h	136b	1:30:53.960	30:18:04.31	20.26
115	k	239b	1:31:13.170	30:23:29.30	20.27
116	h	128b	1:30:53.080	30:17:44.05	20.28
117	f	58b	1:30:37.800	30:23:48.86	20.30
118	i	21b	1:30:22.200	30:12:18.06	20.32
119	n	103b	1:30:45.660	30:26:25.22	20.38
120	f	55b	1:30:37.100	30:25:22.53	20.40
121	n	82b	1:30:44.290	30:26:15.80	20.41
122	b	193b	1:31:02.690	30:24:59.53	20.42
123	h	75b	1:30:43.980	30:16:47.91	20.45
124	q	50b	1:30:31.570	30:16:36.74	20.45
125	n	145b	1:30:54.840	30:29:16.22	20.48
126	h	134b	1:30:53.600	30:17:37.93	20.49
127	d	217b	1:31:08.490	30:20:06.23	20.50
128	l	233b	1:31:11.760	30:28:31.41	20.51

TABLE 2—*Continued*

#	Field	ID	r.a. (1950)	dec. (1950)	V[a]
129	i	20b	1:30:22.090	30:12:13.79	20.52
130	l	268b	1:31:25.250	30:27:07.29	20.57
131	n	90b	1:30:44.540	30:26:14.03	20.58
132	g	100b	1:30:45.330	30:21:06.29	20.58
133	n	96b	1:30:44.840	30:25:54.77	20.61
134	b	183b	1:30:58.970	30:23:56.69	20.62
135	d	174b	1:30:56.360	30:21:17.86	20.63
136	m	144b	1:30:54.830	30:29:16.17	20.63
137	n	125b	1:30:52.240	30:26:29.79	20.64
138	f	57b	1:30:37.660	30:23:38.22	20.66
139	f	56b	1:30:37.500	30:23:41.54	20.67
140	q	48b	1:30:31.340	30:17:26.01	20.68
141	q	40b	1:30:26.060	30:17:05.50	20.69
142	n	111b	1:30:46.850	30:27:11.09	20.70
143	q	49b	1:30:31.460	30:16:38.90	20.71
144	n	107b	1:30:46.100	30:26:07.08	20.73
145	l	242b	1:31:16.830	30:26:25.20	20.73
146	q	53b	1:30:34.380	30:16:12.96	20.75
147	n	112b	1:30:47.580	30:28:01.08	20.75
148	g	143b	1:30:54.630	30:21:23.12	20.76
149	h	115b	1:30:49.810	30:17:15.66	20.76
150	d	178b	1:30:57.010	30:20:40.05	20.77
151	i	34b	1:30:24.870	30:14:21.88	20.78
152	o	274b	1:31:28.170	30:18:13.67	20.79
153	h	140b	1:30:54.580	30:16:11.74	20.79
154	o	273b	1:31:28.170	30:18:22.95	20.82
155	g	106b	1:30:46.070	30:21:41.14	20.85
156	f	32b	1:30:24.170	30:23:57.35	20.93
157	l	244b	1:31:16.930	30:26:14.79	20.96
158	o	269b	1:31:25.810	30:18:26.59	21.07
159	q	39b	1:30:26.020	30:17:14.28	21.07
160	b	194b	1:31:02.790	30:25:30.76	21.09
161	o	279b	1:31:31.340	30:18:49.08	21.09
162	a	6b	1:30:12.690	30:25:44.33	21.11
163	q	42b	1:30:28.060	30:15:48.22	21.12
164	n	85b	1:30:44.360	30:26:04.84	21.13
165	h	69b	1:30:41.000	30:16:43.65	21.20
166	n	76b	1:30:43.920	30:26:10.41	21.25
167	a	10b	1:30:14.740	30:24:31.93	21.26
168	i	26b	1:30:22.910	30:14:52.80	21.28
169	n	80b	1:30:44.170	30:26:19.55	21.29
170	a	11b	1:30:14.770	30:24:37.82	21.29
171	f	45b	1:30:29.090	30:25:52.80	21.30
172	h	78b	1:30:44.120	30:18:20.94	21.33
173	n	109b	1:30:46.380	30:26:01.38	21.38
174	a	1b	1:30:06.400	30:24:10.44	21.40
175	q	43b	1:30:28.130	30:15:50.71	21.42
176	a	4b	1:30:11.180	30:23:38.62	21.51
177	l	243b	1:31:16.900	30:26:18.74	21.55

TABLE 2—*Continued*

#	Field	ID	r.a. (1950)	dec. (1950)	V[a]
178	h	166b	1:30:56.010	30:17:46.71	21.55
179	o	266b	1:31:25.000	30:18:24.81	21.60
180	n	121b	1:30:51.190	30:26:12.83	21.63
181	s	44b	1:30:29.080	30:25:52.90	21.67
182	q	41b	1:30:26.100	30:17:10.16	21.73
183	n	86b	1:30:44.390	30:26:12.95	21.73
184	o	277b	1:31:30.300	30:18:22.94	21.76
185	n	101b	1:30:45.330	30:26:28.62	21.76
186	d	225b	1:31:09.930	30:19:15.34	21.79
187	o	275b	1:31:28.230	30:18:17.08	21.88
188	o	278b	1:31:30.490	30:18:23.15	21.89
189	n	94b	1:30:44.800	30:26:13.46	21.97
190	n	102b	1:30:45.620	30:26:16.45	21.97
191	p	262b	1:31:24.540	30:18:20.88	22.25
192	k	230b	1:31:11.010	30:25:23.71	22.28
193	s	37b	1:30:25.680	30:29:41.66	22.35
194	a	3b	1:30:09.740	30:26:07.90	22.42
195	l	249b	1:31:17.150	30:26:35.15	22.69
196	a	8b	1:30:13.780	30:25:49.87	22.71
197	a	7b	1:30:13.160	30:24:30.23	22.74
198	a	5b	1:30:12.530	30:25:42.27	22.84
199	l	250b	1:31:17.240	30:26:27.37	23.18
200	l	256b	1:31:23.430	30:29:46.33	23.24
201	l	253b	1:31:21.750	30:26:58.81	23.30
202	g	110b	1:30:46.580	30:21:06.82	23.70
203	q	52b	1:30:33.130	30:16:57.88	24.11
204	n	152b	1:30:55.410	30:29:31.02	24.44
205	q	46b	1:30:29.850	30:17:51.65	25.02
206	l	259b	1:31:24.150	30:26:37.55	···
207	n	95b	1:30:44.810	30:26:25.66	···
208	o	276b	1:31:30.140	30:18:22.46	···
209	h	67b	1:30:40.800	30:16:24.96	···
210	o	272b	1:31:27.980	30:18:18.06	···
211	n	124b	1:30:52.120	30:26:31.57	···
212	n	123b	1:30:51.440	30:27:35.83	···
213	l	223b	1:31:09.580	30:25:52.09	···
214	d	224b	1:31:09.890	30:19:20.45	···
215	f	33b	1:30:24.530	30:24:06.06	···
216	h	71b	1:30:41.320	30:16:32.94	···
217	k	252b	1:31:21.280	30:23:55.02	···
218	n	122b	1:30:51.290	30:26:15.99	···
219	n	81b	1:30:44.270	30:26:07.21	···
220	h	64b	1:30:38.990	30:16:28.20	···
221	d	171b	1:30:56.080	30:21:04.54	···
222	n	93b	1:30:44.600	30:26:07.31	···
223	d	164b	1:30:55.790	30:20:54.89	···
224	m	215b	1:31:08.240	30:26:56.14	···
225	n	91b	1:30:44.540	30:26:11.63	···
226	k	232b	1:31:11.260	30:22:46.30	···

TABLE 2—*Continued*

#	Field	ID	r.a. (1950)	dec. (1950)	V[a]
227	h	167b	1:30:56.020	30:17:53.68	···
228	i	35b	1:30:25.310	30:11:48.13	···
229	m	188b	1:31:01.460	30:25:58.88	···
230	m	216b	1:31:08.280	30:26:52.75	···
231	m	170b	1:30:55.950	30:29:16.20	···
232	i	27b	1:30:22.920	30:15:05.03	···
233	c	204b	1:31:04.930	30:17:42.89	···
234	m	214b	1:31:08.200	30:26:49.57	···
235	m	148b	1:30:55.290	30:29:10.64	···
236	l	220b	1:31:09.200	30:27:05.42	···
237	m	146b	1:30:55.160	30:29:13.27	···
238	m	154b	1:30:55.440	30:29:15.05	···
239	d	173b	1:30:56.290	30:21:25.96	···
240	m	158b	1:30:55.560	30:29:10.68	···
241	m	211b	1:31:06.870	30:25:54.27	···
242	j	271b	1:31:27.110	30:21:51.32	···
243	f	30b	1:30:23.620	30:23:18.11	···
244	m	168b	1:30:55.900	30:29:25.32	···
245	j	229b	1:31:10.710	30:19:05.49	···
246	q	31b	1:30:24.110	30:18:44.74	···
247	l	248b	1:31:17.150	30:26:25.28	···
248	n	79b	1:30:44.150	30:26:16.77	···
249	n	87b	1:30:44.430	30:26:09.65	···
250	d	151b	1:30:55.480	30:21:09.59	···
251	l	237b	1:31:12.640	30:28:34.48	···
252	q	24b	1:30:22.570	30:19:13.32	···
253	n	147b	1:30:55.170	30:29:13.17	···
254	l	255b	1:31:23.250	30:29:46.81	···
255	n	88b	1:30:44.450	30:26:07.43	···
256	l	246b	1:31:17.100	30:26:23.48	···
257	j	247b	1:31:17.170	30:22:28.41	···
258	n	163b	1:30:55.660	30:29:27.08	···
259	q	29b	1:30:23.540	30:18:47.33	···
260	m	161b	1:30:55.640	30:29:26.95	···
261	k	258b	1:31:23.700	30:24:56.03	···
262	f	22b	1:30:22.110	30:23:54.13	···
263	h	118b	1:30:50.040	30:17:10.48	···
264	h	114b	1:30:48.480	30:16:40.18	···
265	h	77b	1:30:44.030	30:16:50.06	···
266	m	156b	1:30:55.500	30:29:24.79	···
267	k	241b	1:31:13.280	30:23:18.30	···
268	p	261b	1:31:24.510	30:18:23.99	···
269	l	257b	1:31:23.560	30:29:48.45	···
270	h	70b	1:30:41.030	30:16:25.64	···
271	m	234b	1:31:11.790	30:28:31.90	···
272	m	176b	1:30:56.890	30:27:26.12	···
273	j	260b	1:31:24.380	30:19:27.54	···
274	d	219b	1:31:08.950	30:20:01.43	···
275	m	181b	1:30:58.590	30:29:20.19	···

TABLE 2—*Continued*

#	Field	ID	r.a. (1950)	dec. (1950)	V[a]
276	d	228b	1:31:10.460	30:19:13.57	···
277	n	108b	1:30:46.130	30:26:29.19	···
278	j	270b	1:31:26.280	30:21:51.02	···
279	q	12b	1:30:20.240	30:19:28.24	···

[a]V magnitude, calculated from the continuum at 6100 Å.

TABLE 3. CROSS-CORRELATION: CANDIDATES – WOLF-RAYET STARS

#[a]	ID	W-R[b]	r.a. (1950)[c]	dec. (1950)[c]	ρ[d]
32	25e	MC20	1:30:26.30	30:29:39.0	2″.83
41	107e	MCMS12	1:31:03.03	30:28:28.8	2″.44
219	81b	MC29	1:30:44.10	30:26:07.0	2″.21
189	94b	MC31	1:30:44.80	30:26:12.0	1″.45
133	96b	MCMS04	1:30:44.85	30:25:54.6	0″.21
55	133b	MC44	1:30:53.40	30:17:55.0	2″.47
208	276b	MCMS15	1:31:30.20	30:18:25.3	2″.95
184	277b	MCMS15	1:31:30.20	30:18:25.3	2″.69

[a]Sequential number from Tables 1 and 2
[b]MC = Massey & Conti 1983, MCMS = Massey, Conti, Moffat & Shara 1987
[c]Equatorial coordinates of the W-R stars
[d]separation between the candidate and the W-R star

TABLE 4. CROSS-CORRELATION: CANDIDATES – SNRs – X-RAY SOURCES

#[a]	ID	SNR[b]	ρ[c]	X-PSPC[d]	ρ[c]	X-HRI[e]	ρ[c]
153	1e	004+228	9.7	RP05	6.3	RH01	12.1
31	3e	004+226	13.1	RP05	21.4	RH01	19.8
130	17e	022+190	1.3	...	...	...	...
32	25e	...	...	RP14	16.9	...	...
133	86e	...	...	RP24	29.3	RH14	13.5
1	95e	100+241	11.8	...	...	...	...
120	103e	102+285	12.4	...	...	...	...
41	107e	102+285	14.1	...	...	...	...
119	124e	113+157	1.3	...	...	...	...
42	144e	...	...	RP36	18.3	...	...
167	10b	015+245	3.9	...	...	...	...
170	11b	015+245	8.4	...	...	...	...
252	24b	022+190	15.1	...	...	...	...
75	38b	...	...	RP14	18.5	...	...
123	75b	...	...	RP21	10.0	RH12	15.1
265	77b	...	...	RP21	9.0	RH12	14.0
69	89b	...	...	RP21	11.6	RH12	14.4
63	99b	...	...	RP21	8.5	RH12	6.4
132	100b	...	...	RP22	14.1	RH13	14.8
202	110b	047+211	3.4	RP22	11.7	RH13	6.3
211	124b	053+265	6.7	...	...	...	...
137	125b	053+265	4.7	...	...	...	...
44	126b	053+265	1.4	...	...	...	...
113	127b	053+265	1.6	...	...	...	...
31	141b	054+257	11.4	...	...	...	...
12	182b	059+177	0.7	...	...	...	...
134	183b	100+241	13.6	...	...	...	...
49	190b	...	...	RP28	9.2	RH16	9.2
19	206b	...	...	RP30	8.8	...	...
217	252b	121+239	1.4	...	...	...	...
201	253b	121+271	6.9	RP35	11.9	...	...
206	259b	125+266	12.5	...	...	...	...
79	267b	125+192	3.3	...	...	...	...
208	276b	130+184	2.6	...	...	...	...
184	277b	130+184	2.4	...	...	...	...
188	278b	130+184	4.2	...	...	...	...

[a]Sequential number from Tables 1 and 2
[b]Long et al. 1990, Gordon et al. 1995
[c]separation from the candidate, in arcsec
[d]from ROSAT-PSPC, Long et al. 1995
[e]from ROSAT-HRI, Schulman & Bregman 1995

TABLE 5. CROSS-CORRELATION: CANDIDATES – RADIO SOURCES

#[a]	ID	Radio Source ID[b]	ρ[c]
130	17e	131	1.30
1	95e	82	0.98
119	124e	46	2.91
167	10b	145	1.32
118	21b	138	2.63
215	33b	135	0.91
17	65b	119	2.29
209	67b	114	1.77
47	68b	114	2.49
270	70b	114	1.30
222	93b	110	1.67
93	105b	108	0.68
202	110b	105	2.72
264	114b	166	2.05
149	115b	100	1.94
68	117b	100	1.94
81	119b	100	2.69
44	126b	95	1.17
113	127b	95	1.54
106	129b	93	2.01
22	132b	93	1.69
95	135b	92	1.15
21	139b	90	1.75
238	154b	89	2.69
56	155b	89	2.88
221	171b	87	2.47
239	173b	86	1.96
30	180b	85	2.74
12	182b	84	1.38
134	183b	181	0.95
38	184b	81	1.20
86	186b	78	0.90
54	187b	76	0.83
229	188b	76	0.79
102	192b	73	0.71
65	198b	184	2.96
224	215b	62	1.56
230	216b	62	1.95
60	227b	55	2.30
192	230b	53	2.60
103	231b	53	1.03
128	233b	50	2.50
271	234b	50	2.07
89	245b	42	1.70
256	246b	42	0.75

TABLE 5—*Continued*

#[a]	ID	Radio Source ID[b]	ρ[c]
247	248b	42	1.16
268	261b	33	2.04
191	262b	33	1.68
278	270b	30	2.84
154	273b	25	1.00

[a]Sequential number from Tables 1 and 2
[b]Gordon et al. 1995
[c]separation from the candidate, in arcsec

Figure 1.— B-band image of M 33 (Long *et al.* 1990) with a grid ovelaid showing the position of the 19 fields. The grid is reproduced in the bottom left corner on a reduced scale to show the labels of the fields, from 'a' to 's'.

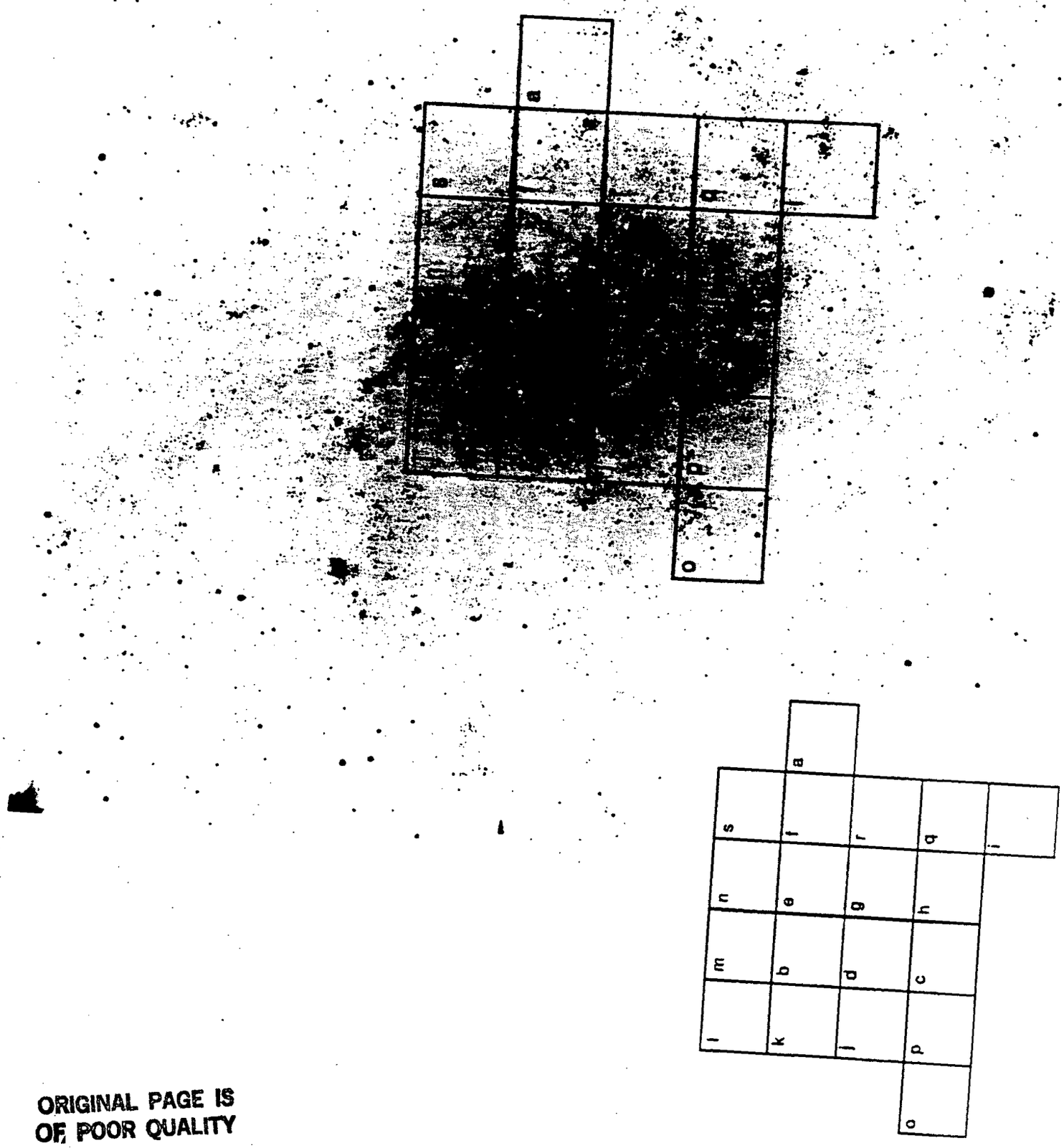

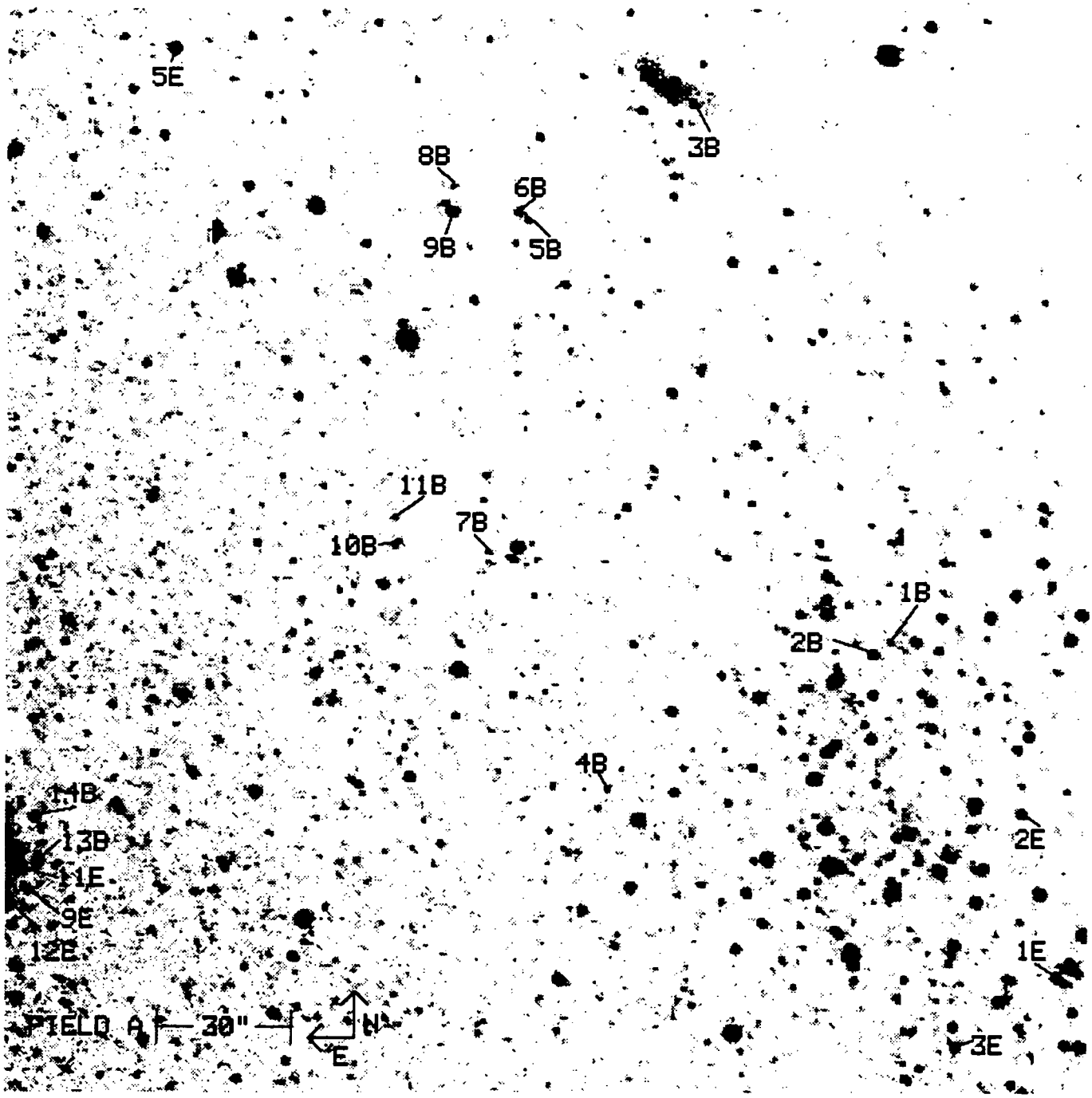

Figure 2.— Finding charts for the 432 compact Hα emitting regions found in the 19 fields of M 33. Line emitting stars have the suffix 'e'. Stars embedded in extendend Hα regions have the suffix 'b'. The scale and the orientation of the fields are also shown.

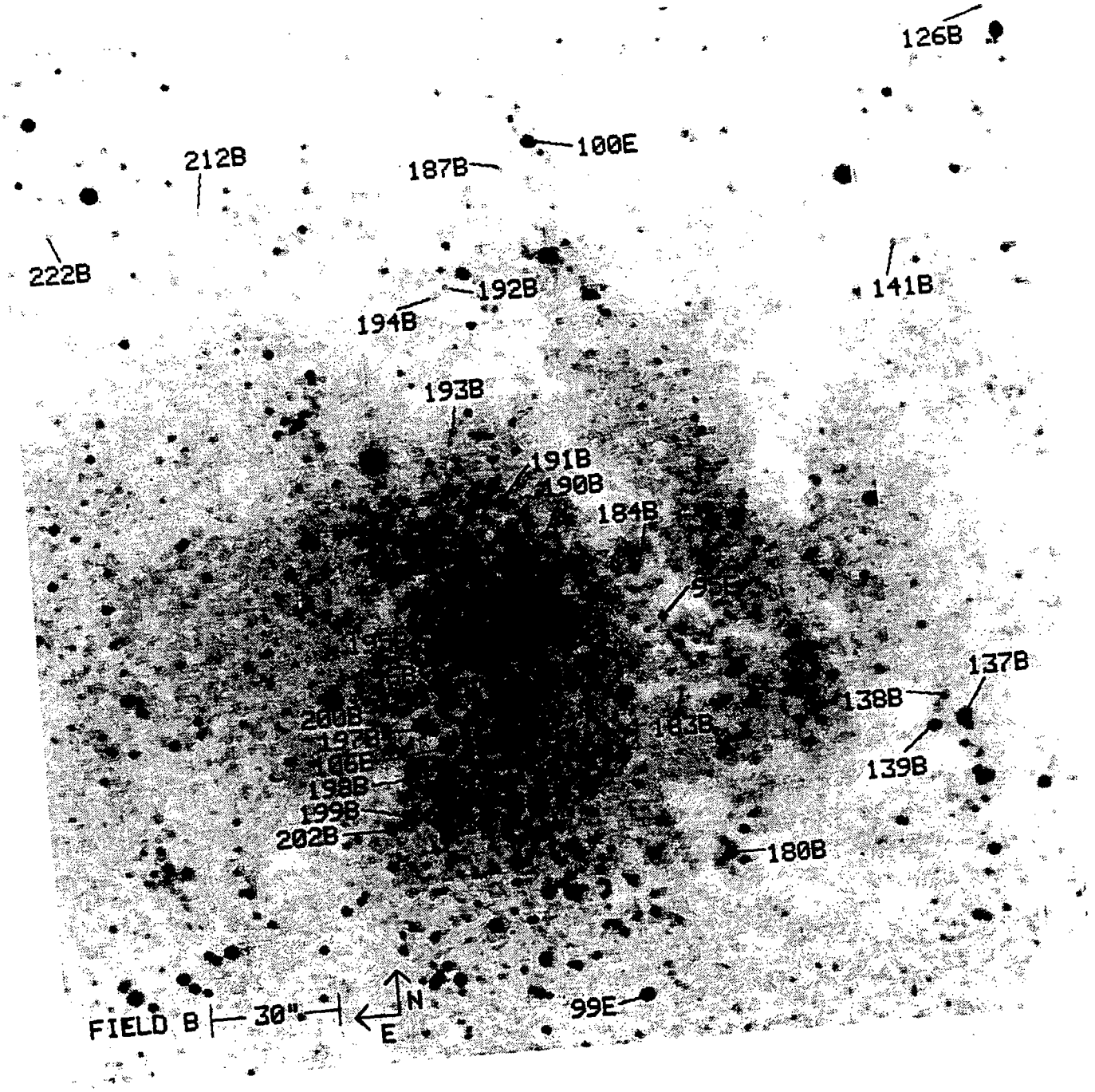

Figure 2.—*Continued*

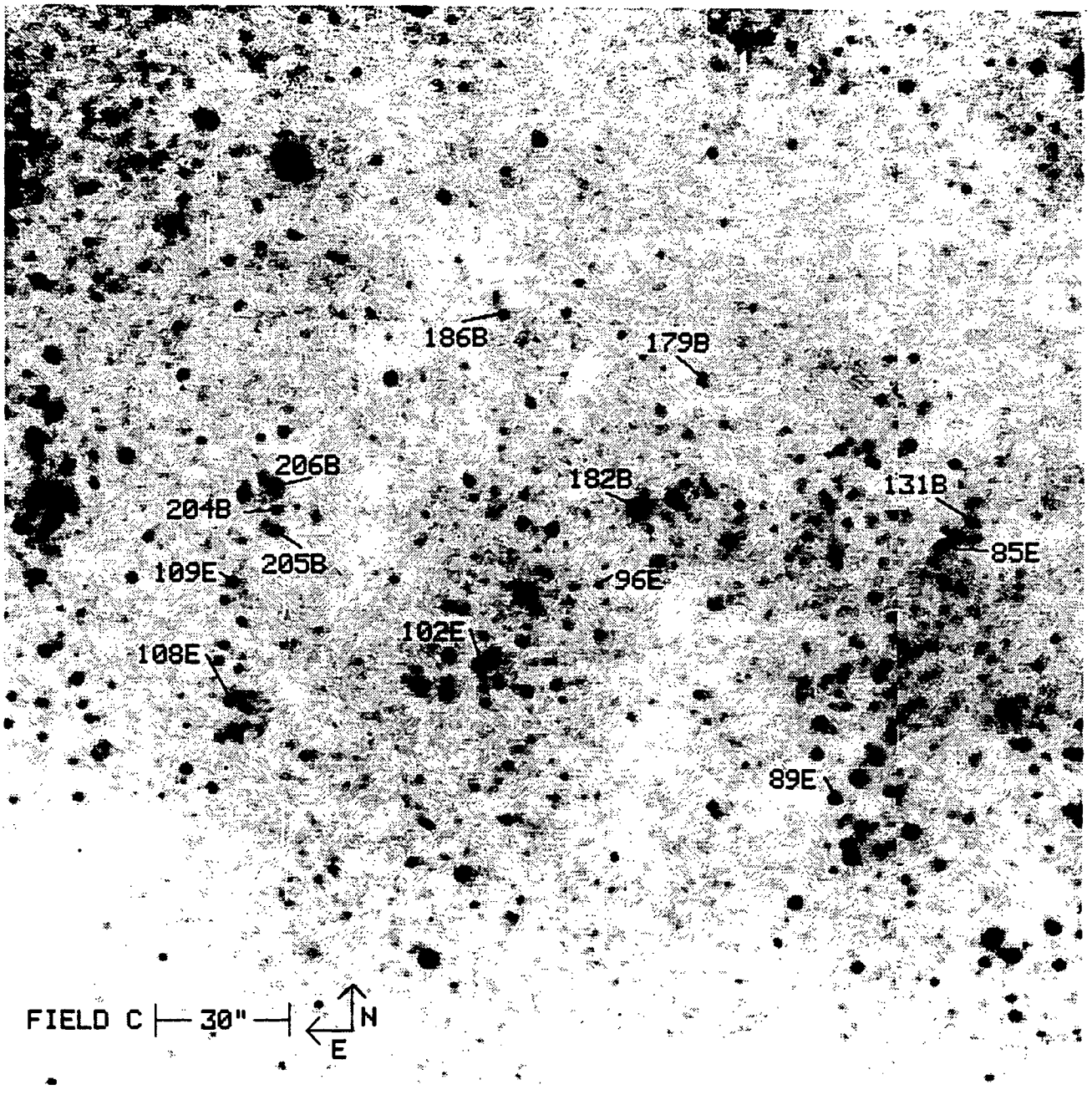

Figure 2.—*Continued*

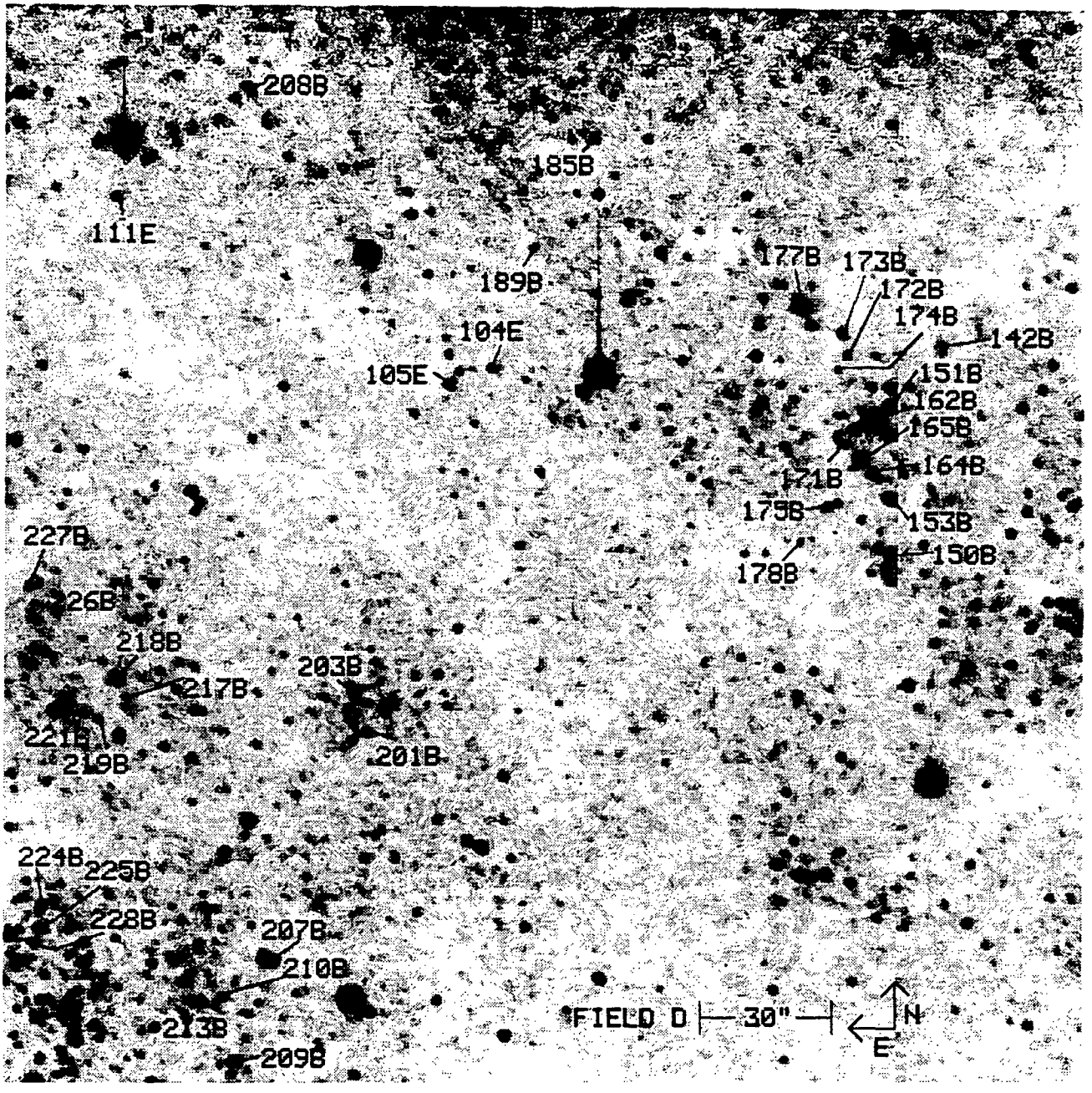

Figure 2.—*Continued*

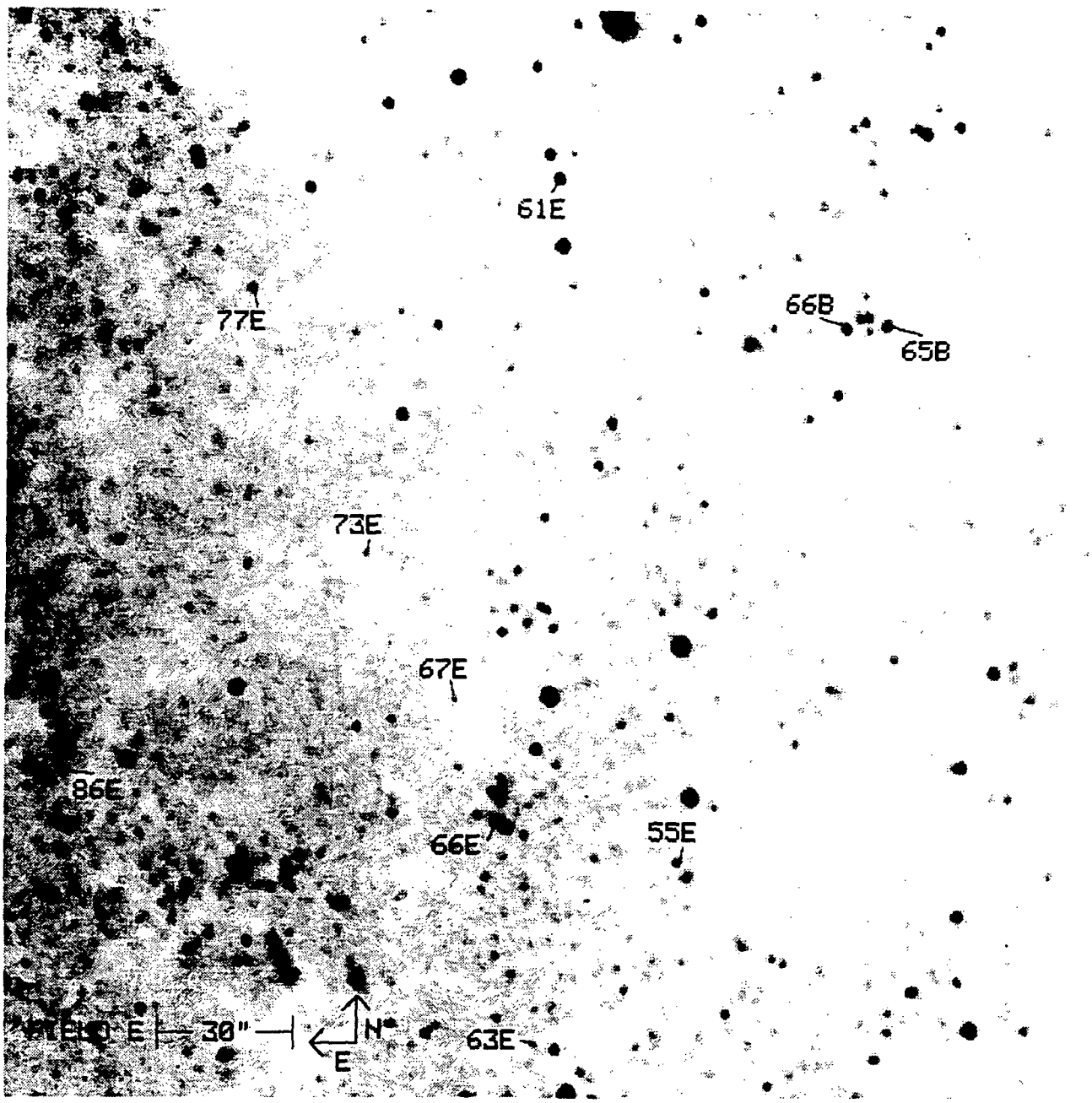

Figure 2.—*Continued*

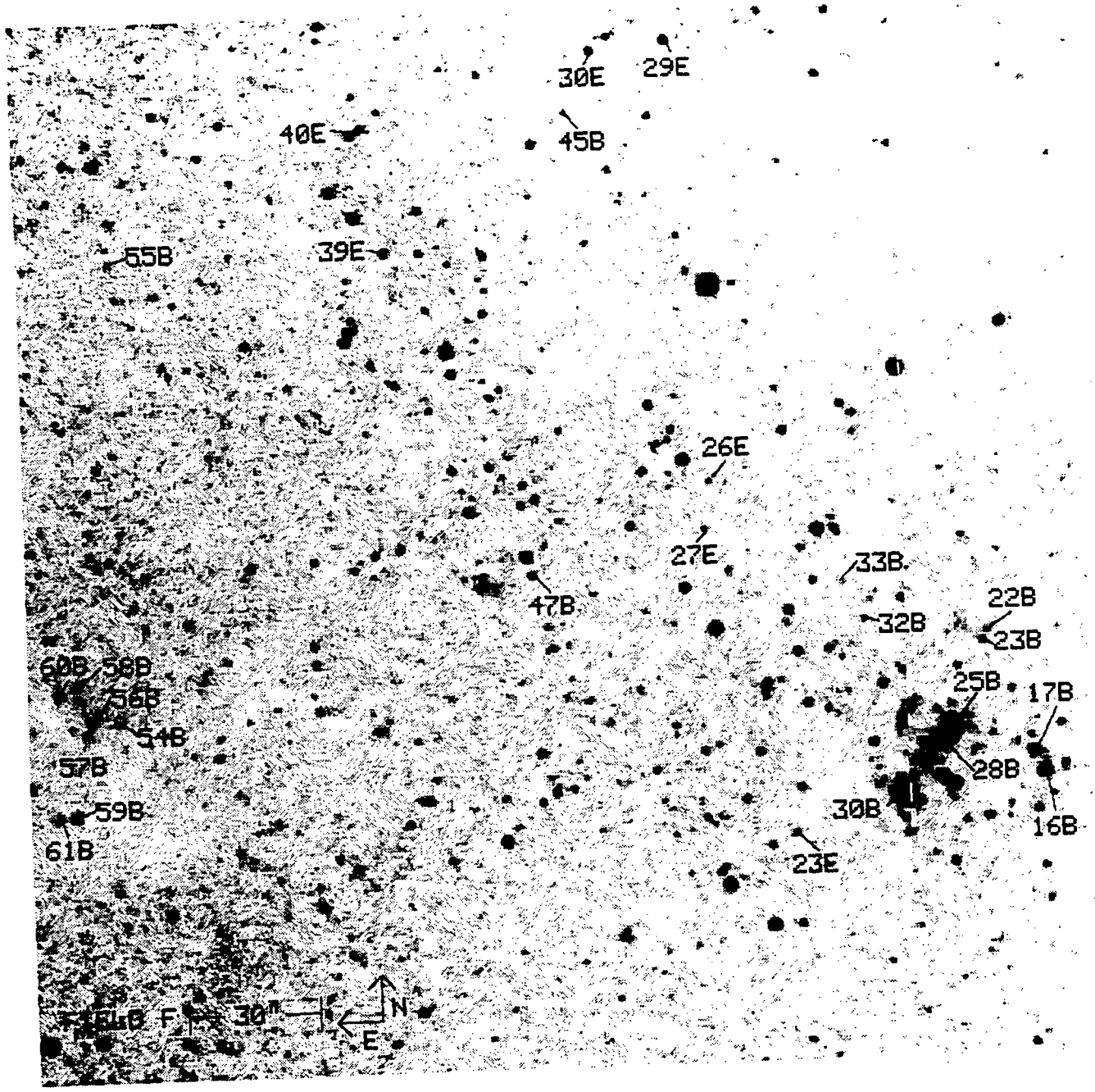

Figure 2.—*Continued*

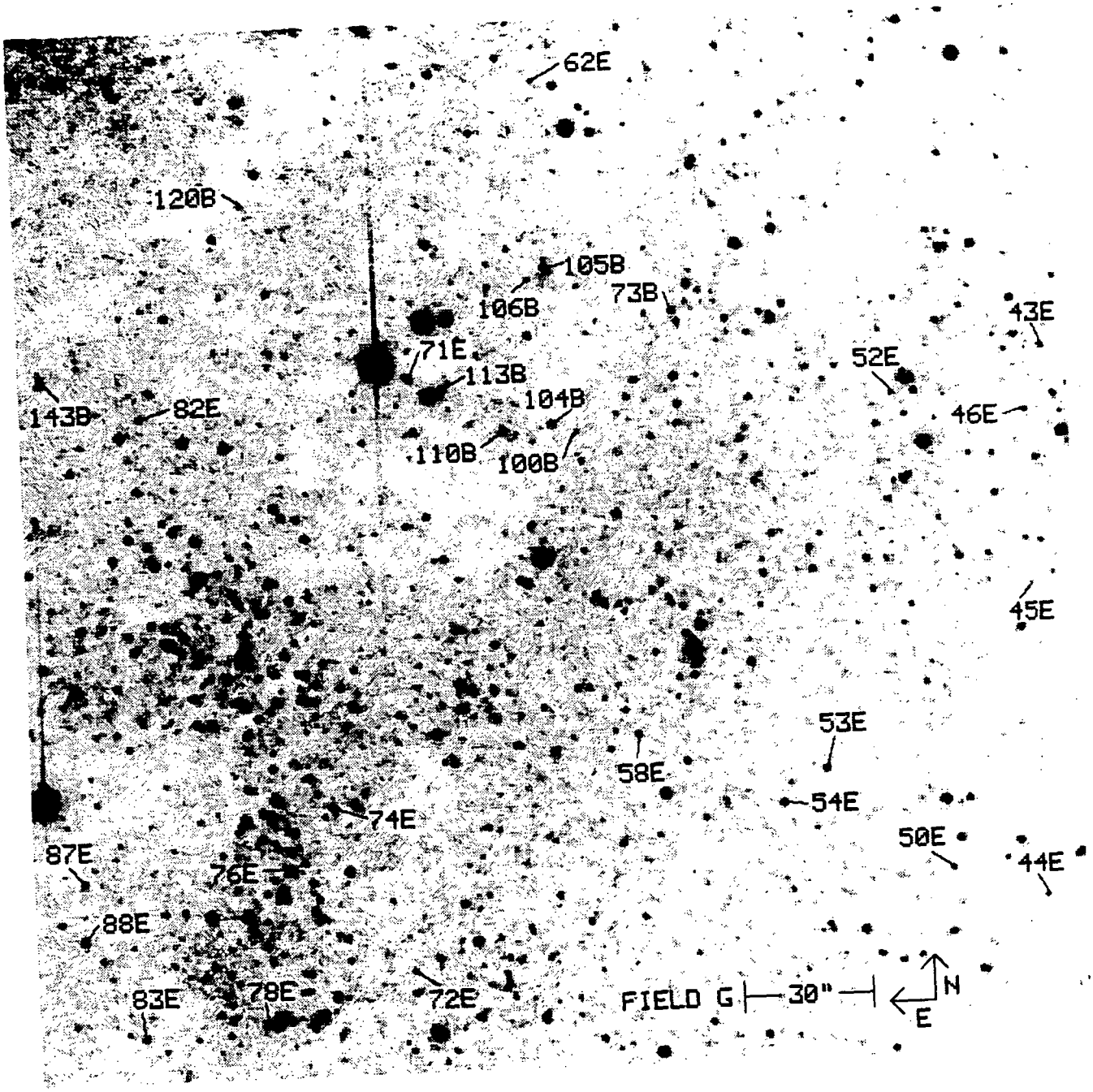

Figure 2.—*Continued*

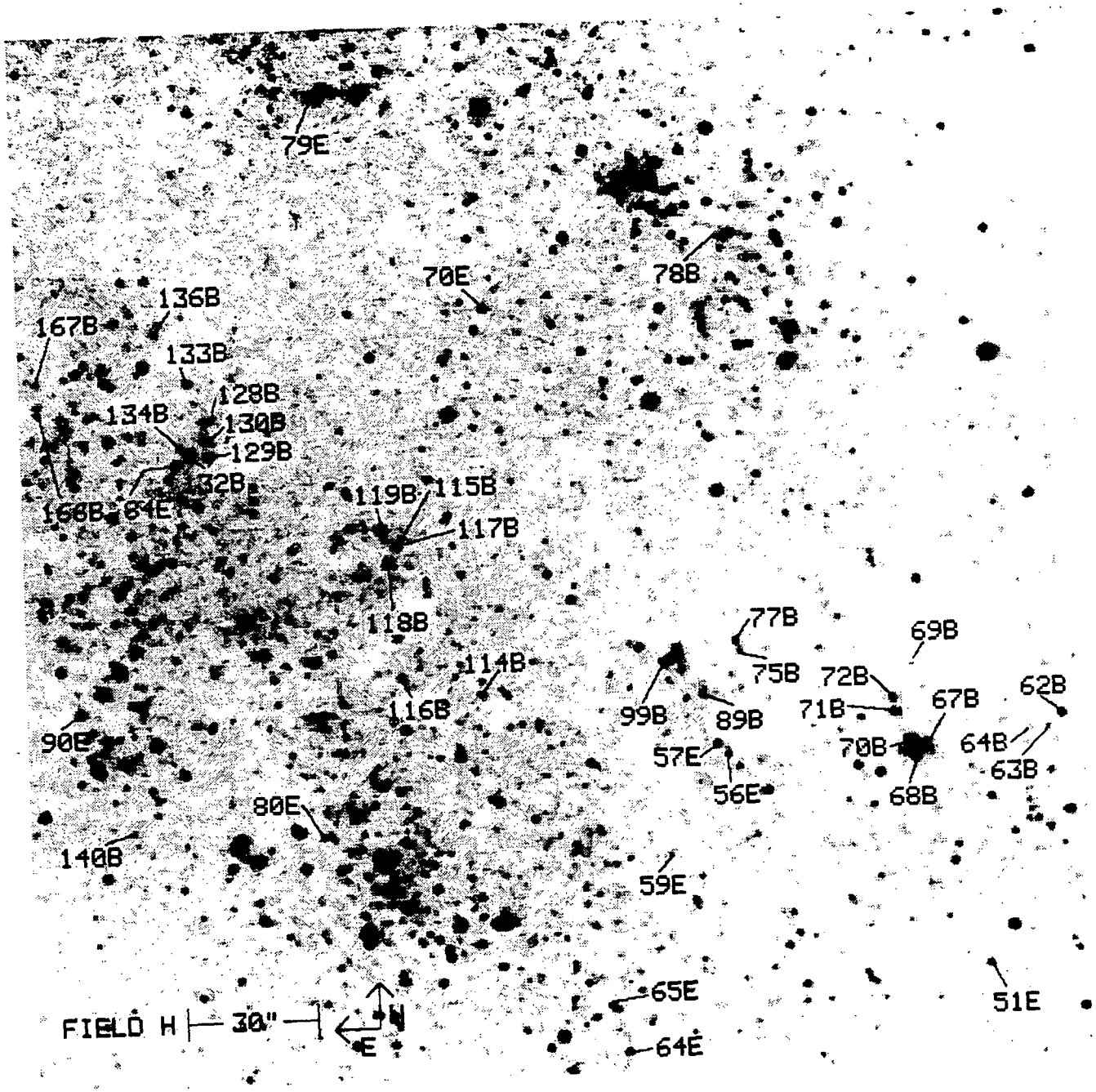

Figure 2.—*Continued*

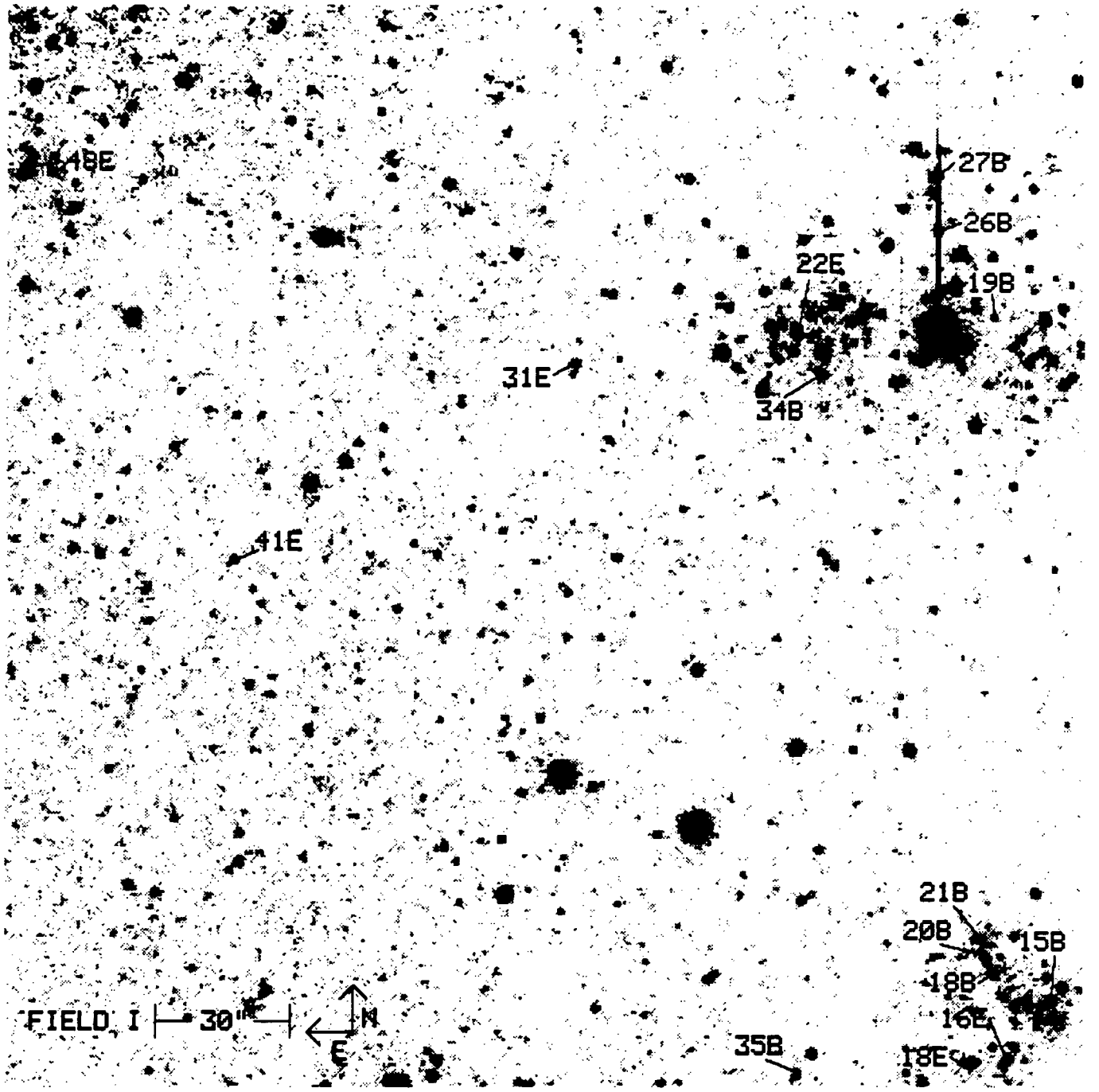

Figure 2.—*Continued*

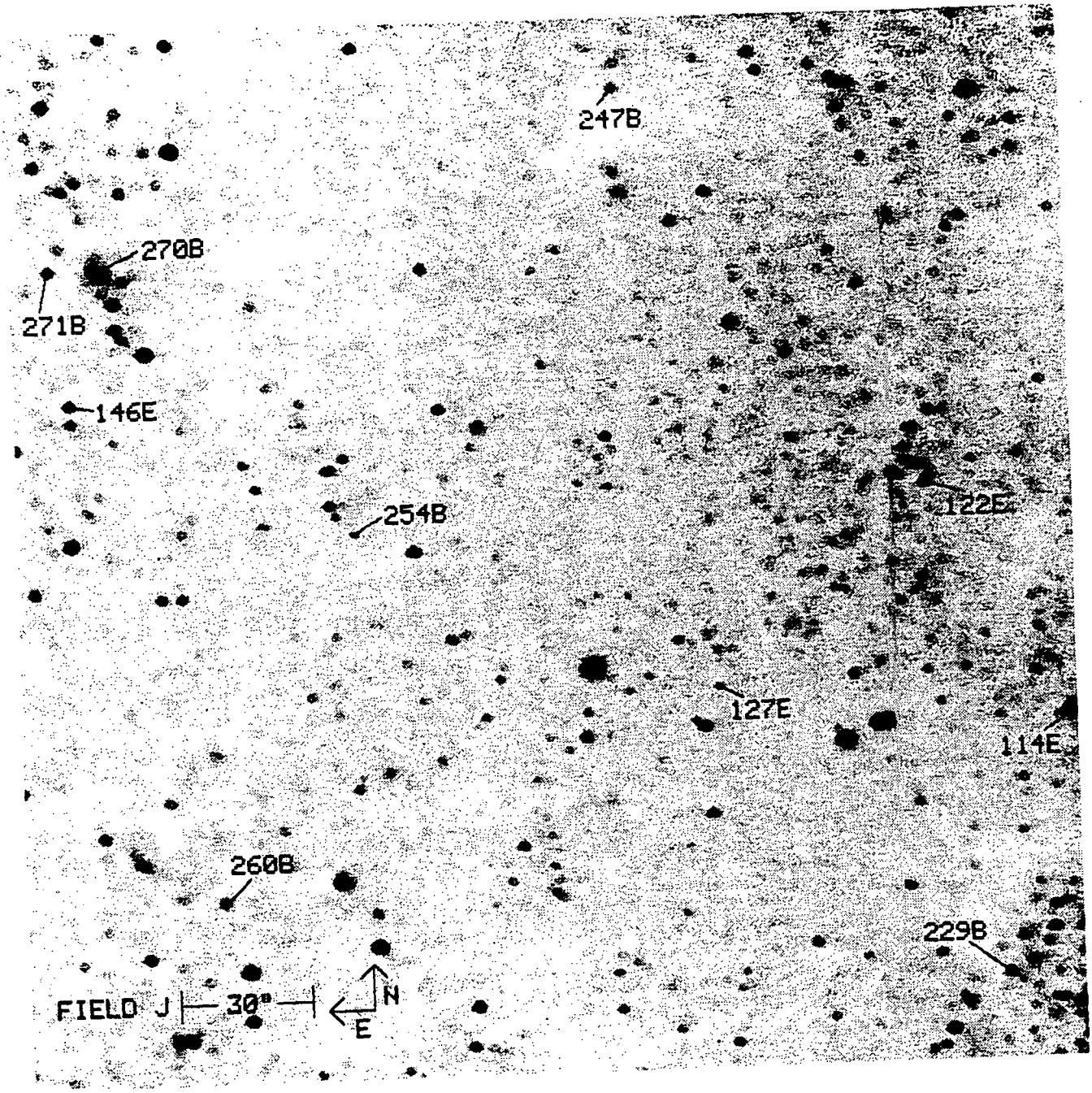

Figure 2.—*Continued*

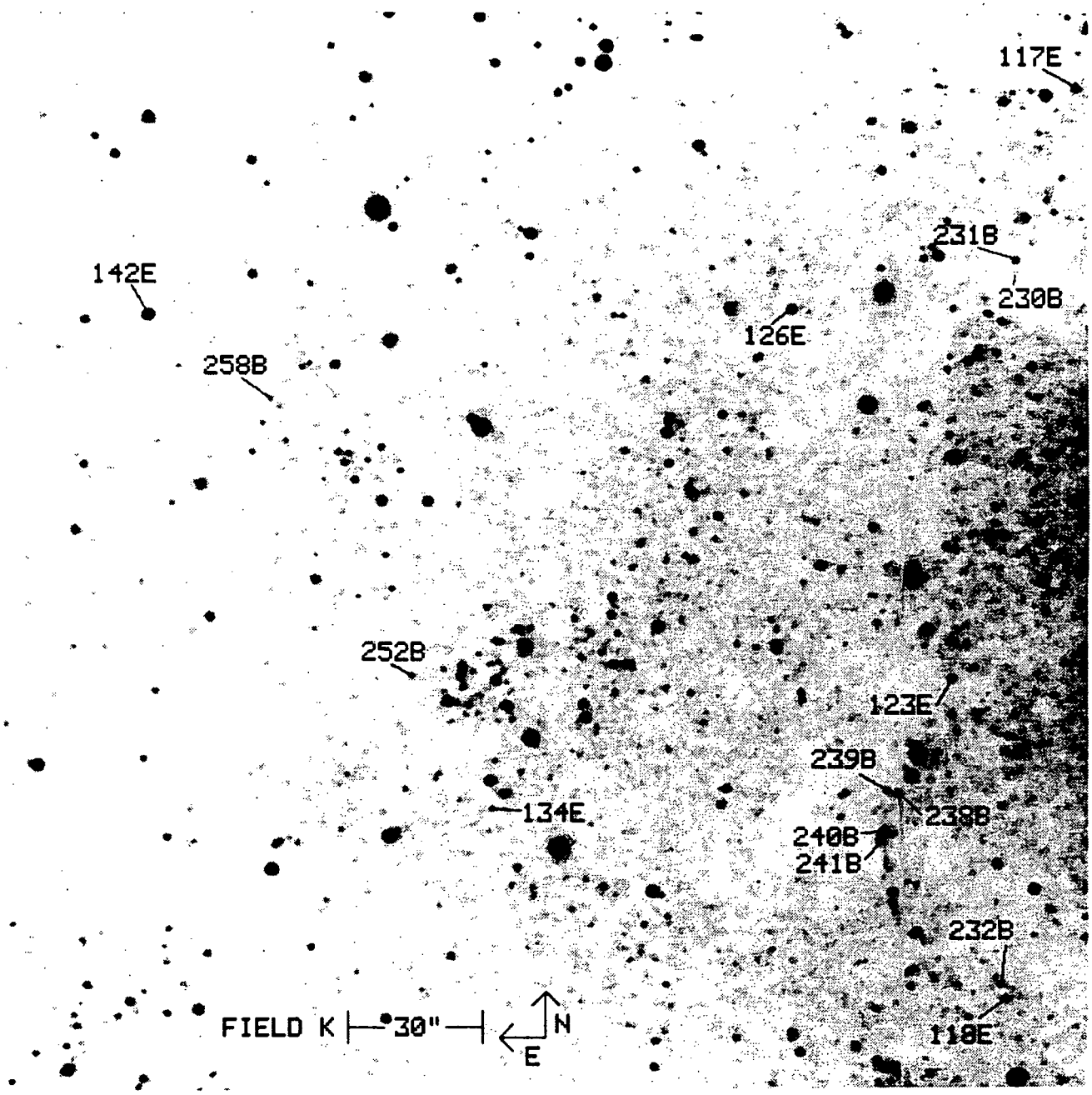

Figure 2.—*Continued*

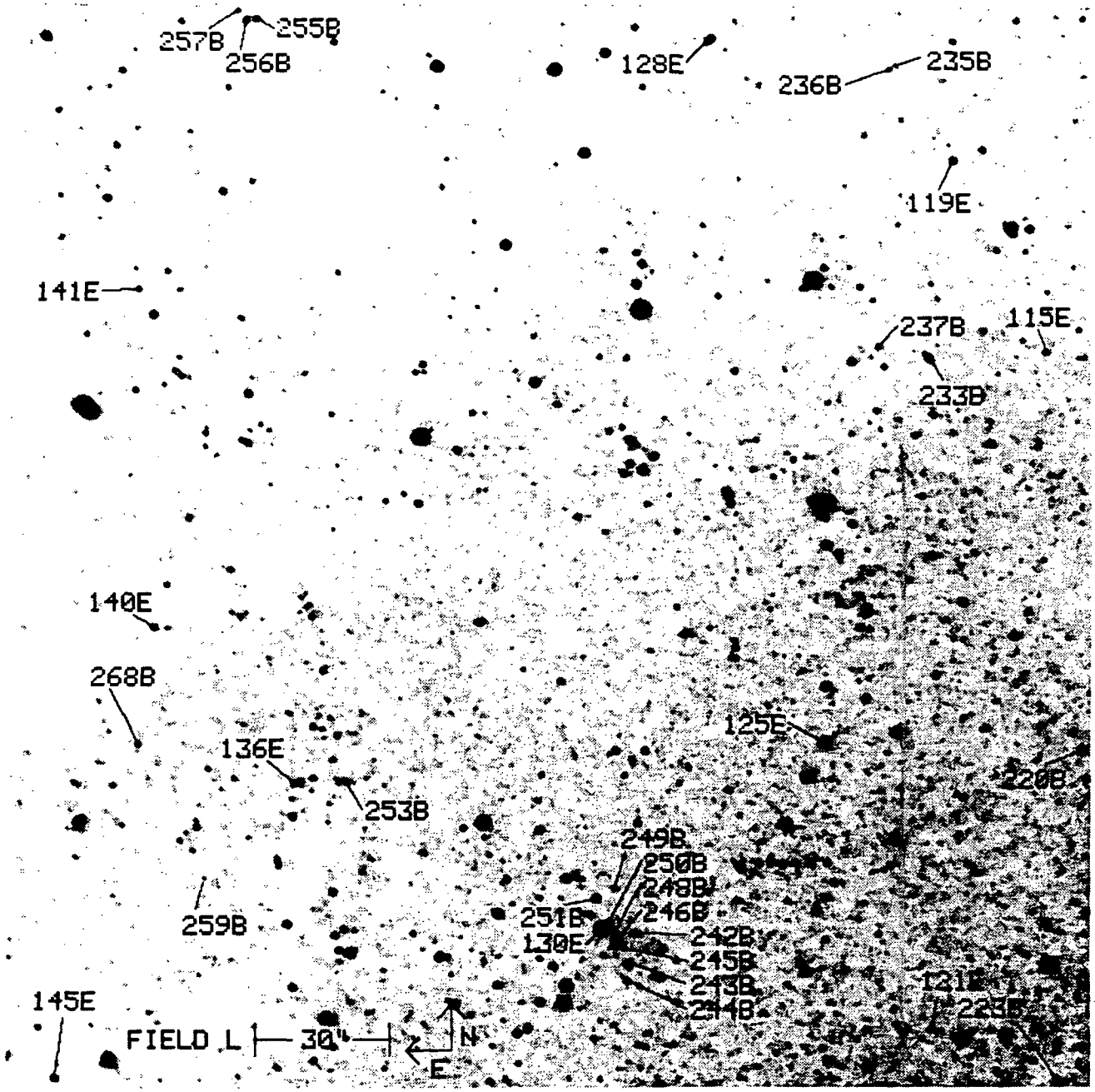

Figure 2.—*Continued*

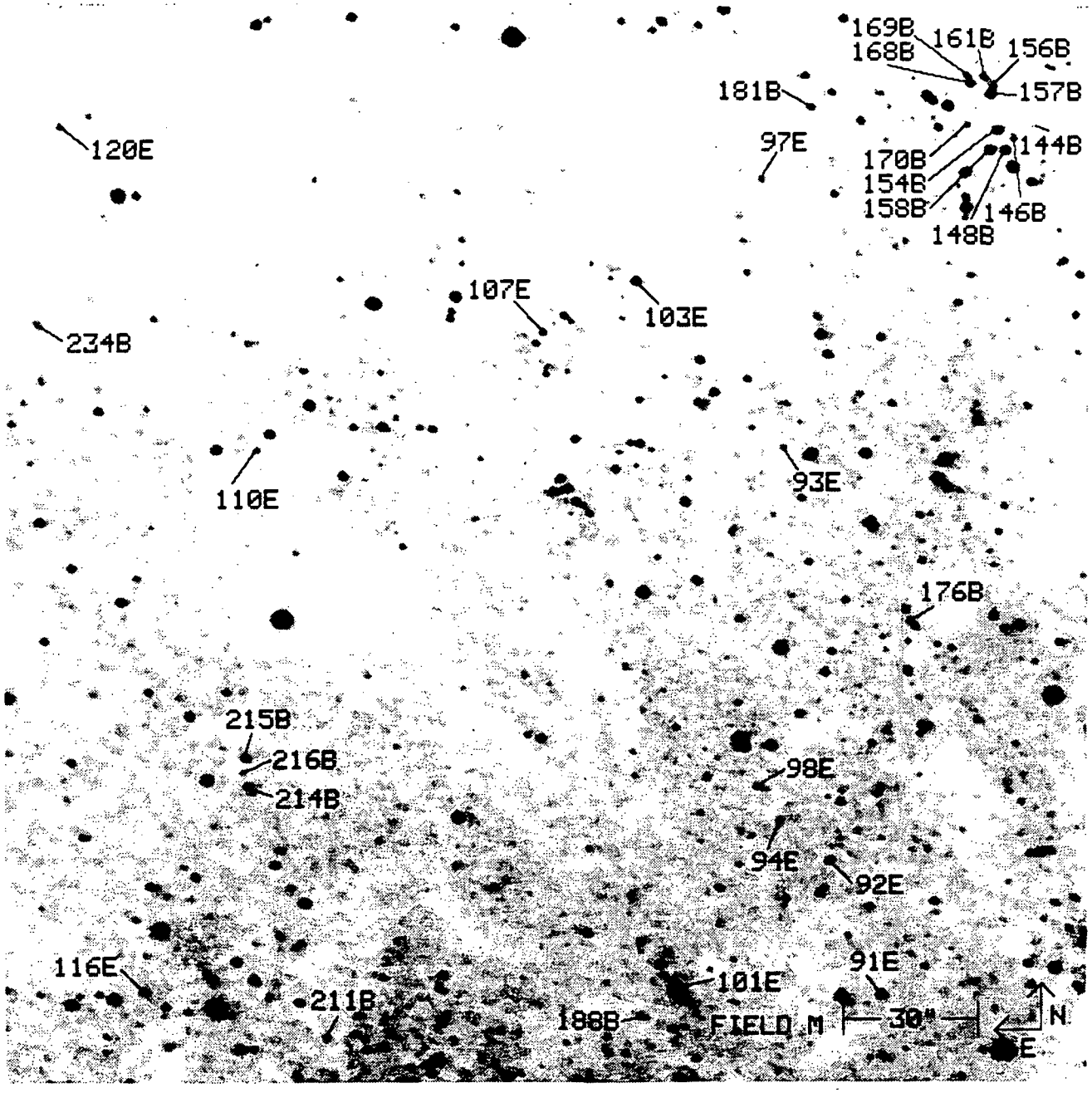

Figure 2.—*Continued*

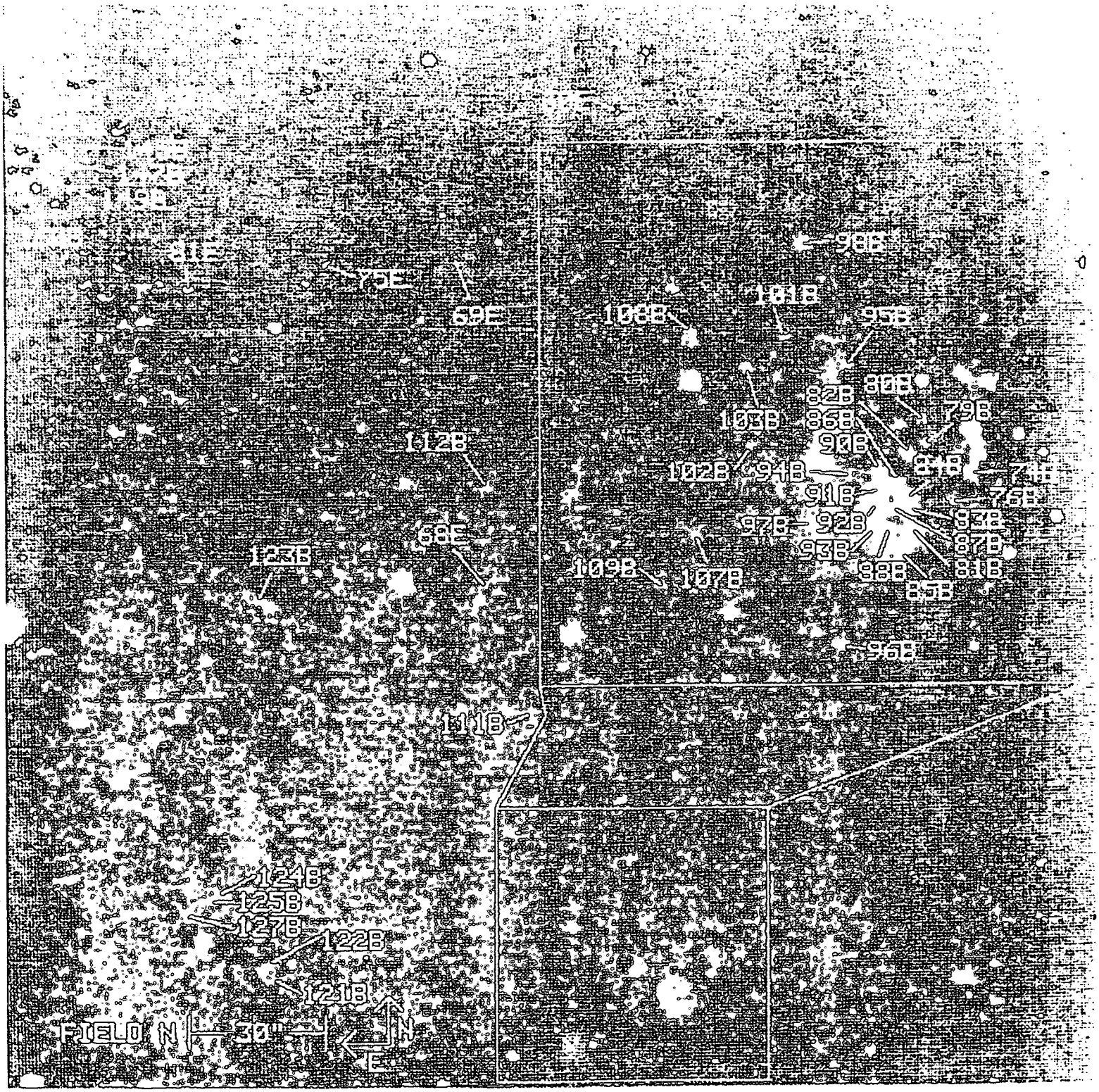

Figure 2.—*Continued*

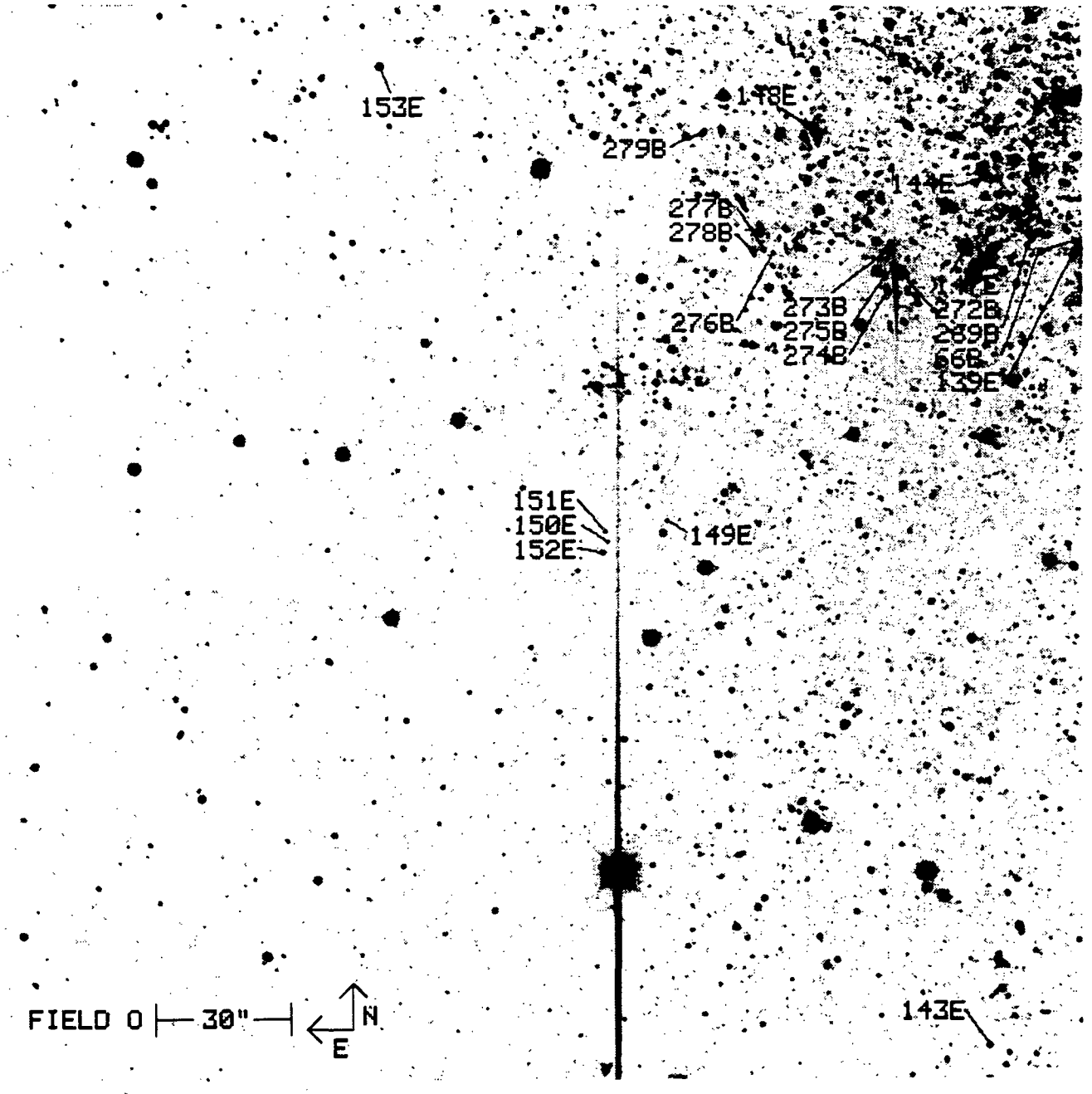

Figure 2.—*Continued*

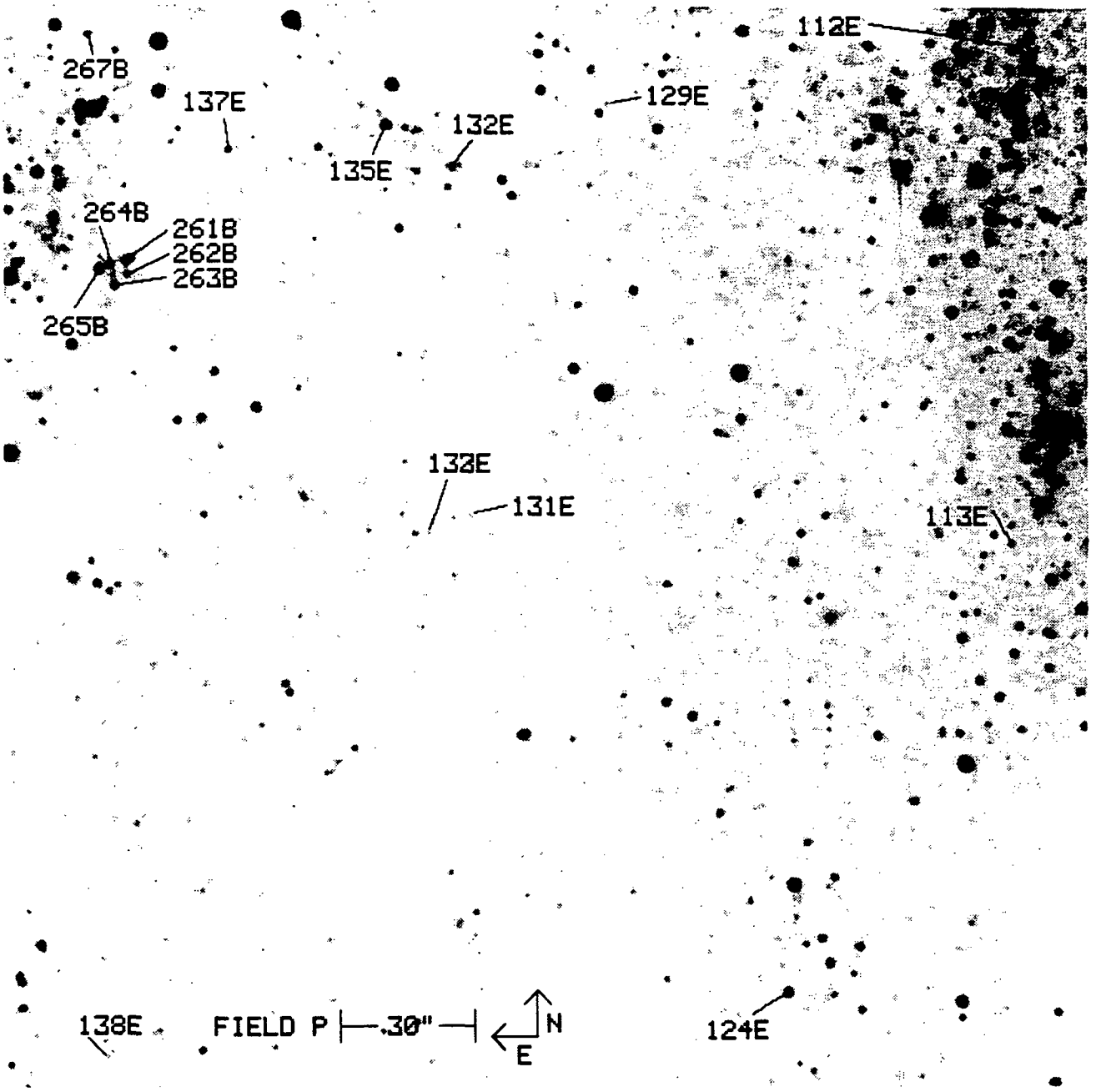

Figure 2.—*Continued*

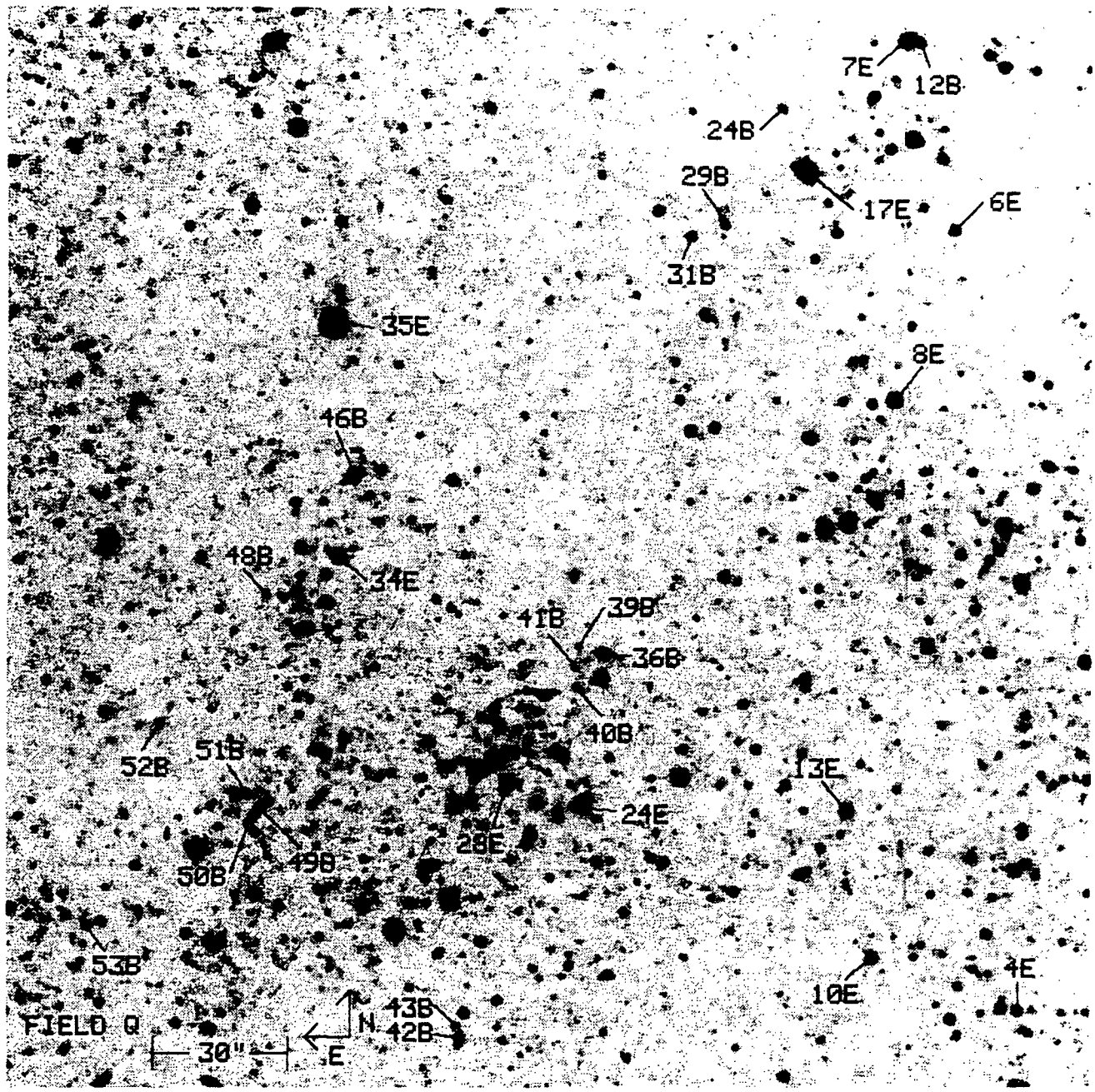

Figure 2.—*Continued*

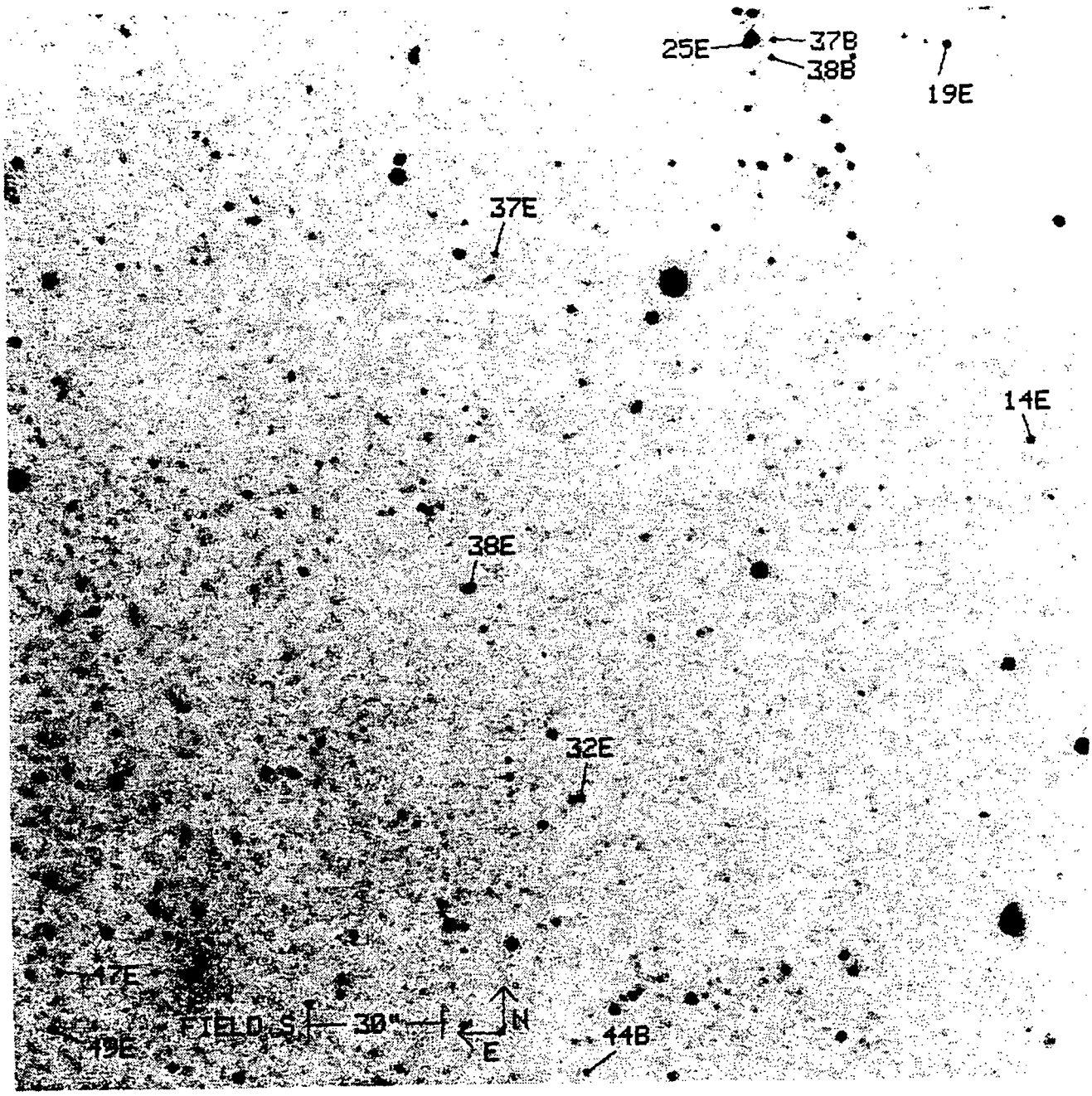

Figure 2.—*Continued*